

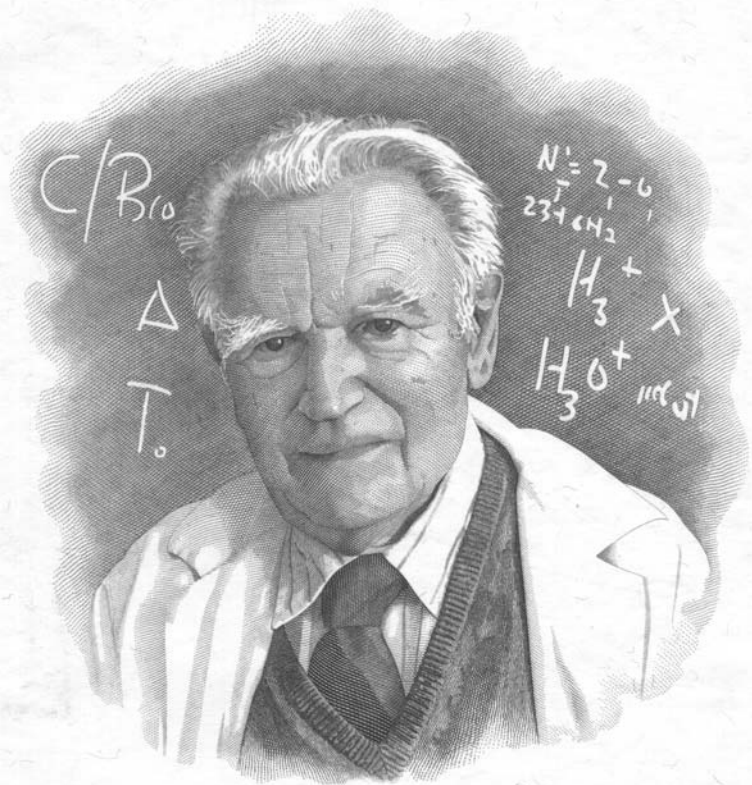
Interstellar Molecules: From Hydrogen to Amino Acids

T. Amano

Department of Chemistry and
Department of Physics and Astronomy
The University of Waterloo

*“Hydrogen is the most
important constituent
of the Universe.”*

G. Herzberg



Gerhard Herzberg

Gerhard Herzberg

Engraved and printed by Canadian Bank Note Company, Limited
Gravé et imprimé par Canadian Bank Note Company, Limited

Photograph courtesy of National Research Council Canada
Photographe courtoisie du Conseil national de recherches Canada

In this talk.....

- Overview of Interstellar Space and Interstellar Molecules

(ex) H_3^+ and HCO^+

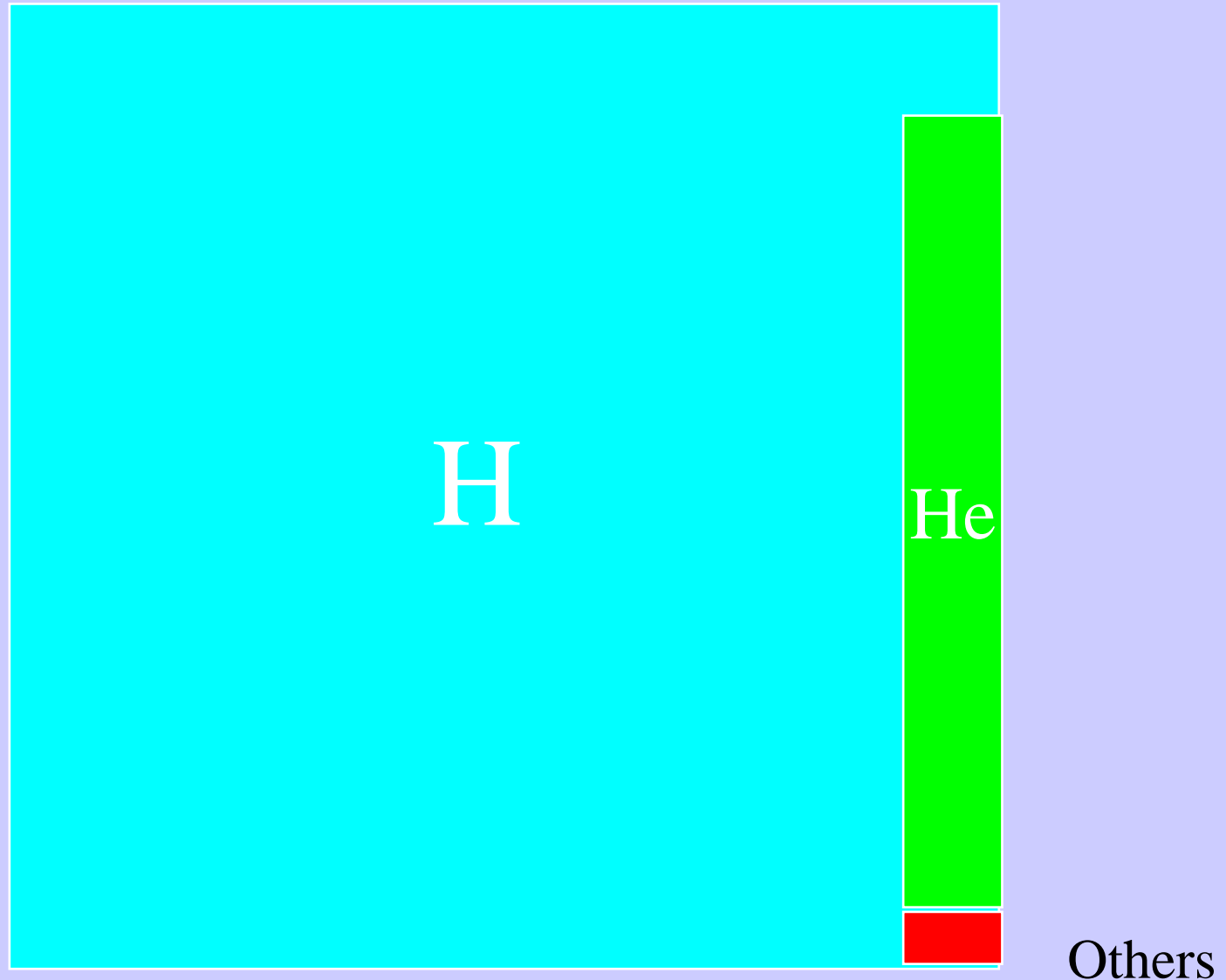
- Submillimeter-wave Spectroscopy and New Initiatives in Submillimeter Astronomy

Multiply deuterated species in space

Anions in the lab and in space

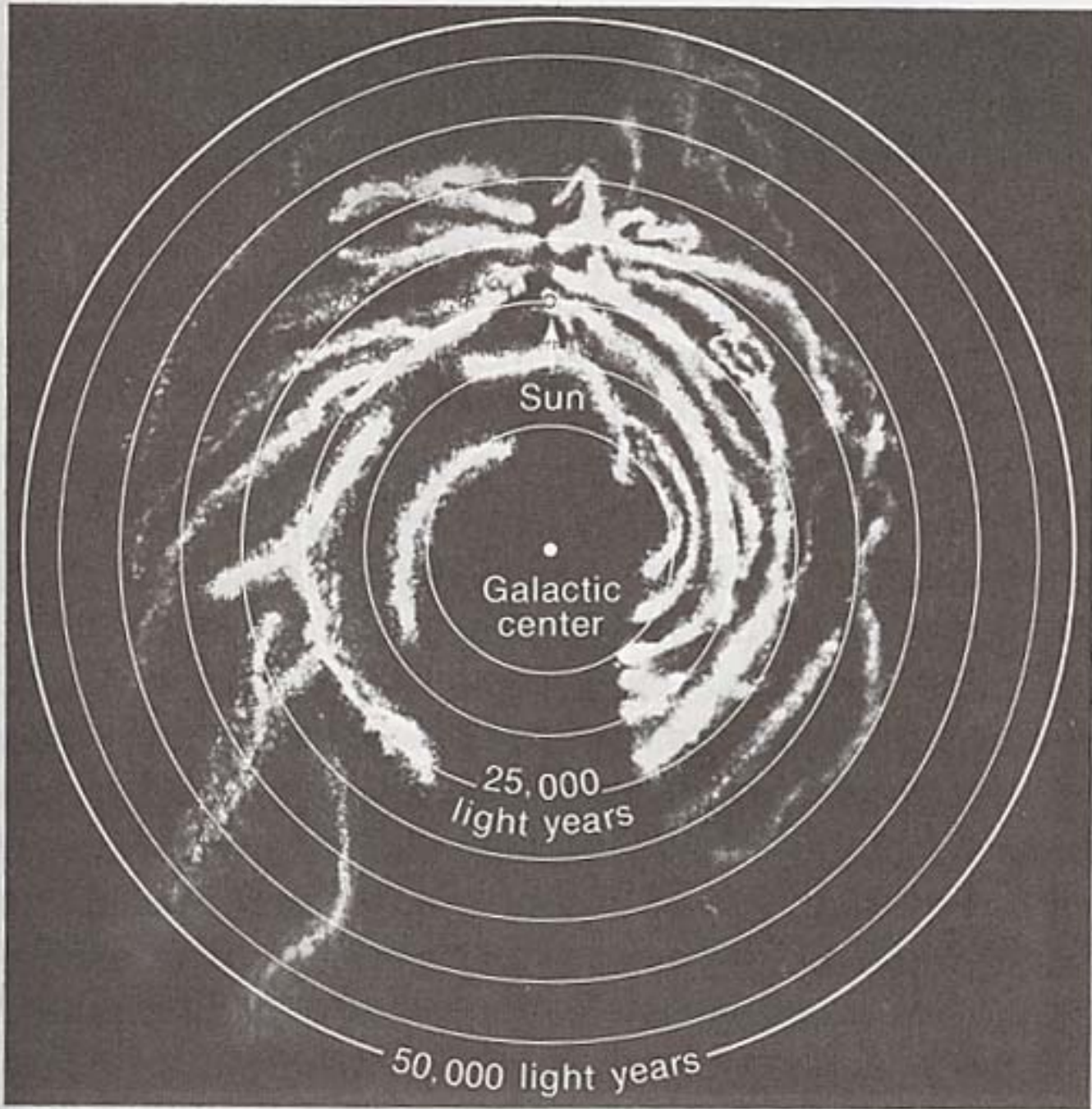
Biological molecules in space

Cosmic Abundance



21cm-Line of Hydrogen Atom

- van de Hulst (Leiden Observatory)
1944 pointed out possibility of H 21cm line.
- Ewen, Purcell (Harvard University)
Oort, Muller (Leiden Observatory)
1951 detection of the line
Christiansen, Hindman (Australia, AAO)
- Hydrogen Maser (N. F. Ramsey)
1 420 405 751.786Hz
21.10611405 cm



© Anglo-Australian Observatory



Discovery of Interstellar Molecules

- 1814 Fraunhofer lines
- 1904 Absorption lines of Ca,K against bright stars
- 1934 Discovery of 4 Diffuse Interstellar Bands (DIBS) Still remain unidentified.
- 1937-1941 Discovery of CH⁺,CH,CN 4230-4300 Å
- 1951 Bates, Spitzer : skeptical about interstellar molecules.
- 1955~ Townes, Shklovsky: Pointed out possibility of observing molecules with radio telescopes.

OH, NH₃, HCN, CO.....

Table 4.1: List of Interstellar Molecules Identified(as of May, 2004).

Simple hydrides, oxides, sulfides, halogenated compounds				
H ₂ (IR)	CO	NH ₃	CS	NaCl*
HF	SiO	SiH ₄ *(IR)	SiS	AlCl*
HCl	SO ₂	C ₂ (IR)	H ₂ S	KCl*
H ₂ O	OCS	CH ₄ *(IR)	PN	AlF*
N ₂ O	CO ₂			
Nitriles, Acetylene derivatives				
C ₃ *(IR)	HCN	CH ₃ CN	HNC	C ₂ H ₄ *(IR)
C ₅ *(IR)	HC ₃ N	CH ₃ C ₃ N	HNCO	C ₂ H ₂ *(IR)
C ₃ O	HC ₅ N	CH ₃ C ₅ N?	HNCS	HC ₄ H*(IR)
C ₃ S	HC ₇ N	CH ₃ C ₂ H	HNCCC	HC ₆ H*(IR)
C ₄ Si*	HC ₉ N	CH ₃ C ₄ H	CH ₃ NC	
	HC ₁₁ N	CH ₃ CH ₂ CN	HCCNC	
	HC ₂ CHO	CH ₂ CHCN		
Aldehydes, Alcohols, Ethers, Ketones, Amides				
H ₂ CO	CH ₃ OH	HCOOH	CH ₂ NH	H ₂ C ₃
H ₂ CS	CH ₃ CH ₂ OH	HCOOCH ₃	CH ₃ NH ₂	H ₂ C ₄
CH ₃ CHO	CH ₃ SH	CH ₃ COOH	NH ₂ CN	H ₂ C ₆
NH ₂ CHO	(CH ₃) ₂ O	CH ₂ OHCHO		
H ₂ CCO	(CH ₃) ₂ CO	CH ₂ CHOH		
Cyclic molecules				
c-C ₃ H ₂	c-SiC ₂	c-SiC ₃ *	c-C ₃ H	c-C ₂ H ₄ O
C ₆ H ₆ *(IR)	c-C ₂ H ₄ S?			
Molecular Ions				
CH ⁺ (Opt)	HCO ⁺	HCNH ⁺	H ₃ O ⁺	HN ₂ ⁺
HCS ⁺	HOCO ⁺	HC ₃ NH ⁺	HOC ⁺	H ₃ ⁺ (IR)
CO ⁺	H ₂ COH ⁺	SO ⁺		H ₂ D ⁺
				D ₂ H ⁺
Free Radicals				
OH	C ₂ H	CN	C ₂ O	C ₂ S
CH	C ₃ H	C ₃ N	NO	NS
CH ₂	C ₄ H	C ₅ N?	SO	SiC*
CH ₃ (IR)	C ₅ H	HCCN*	HCO	SiN*
NH(UV)	C ₆ H	CH ₂ CN	MgNC	CP*
NH ₂	C ₇ H	CH ₂ N	MgCN	SiCN*
SH(IR)	C ₈ H	HNO	NaCN	FeO?
			AiNC	

Molecules identified other than radio are specified individually.

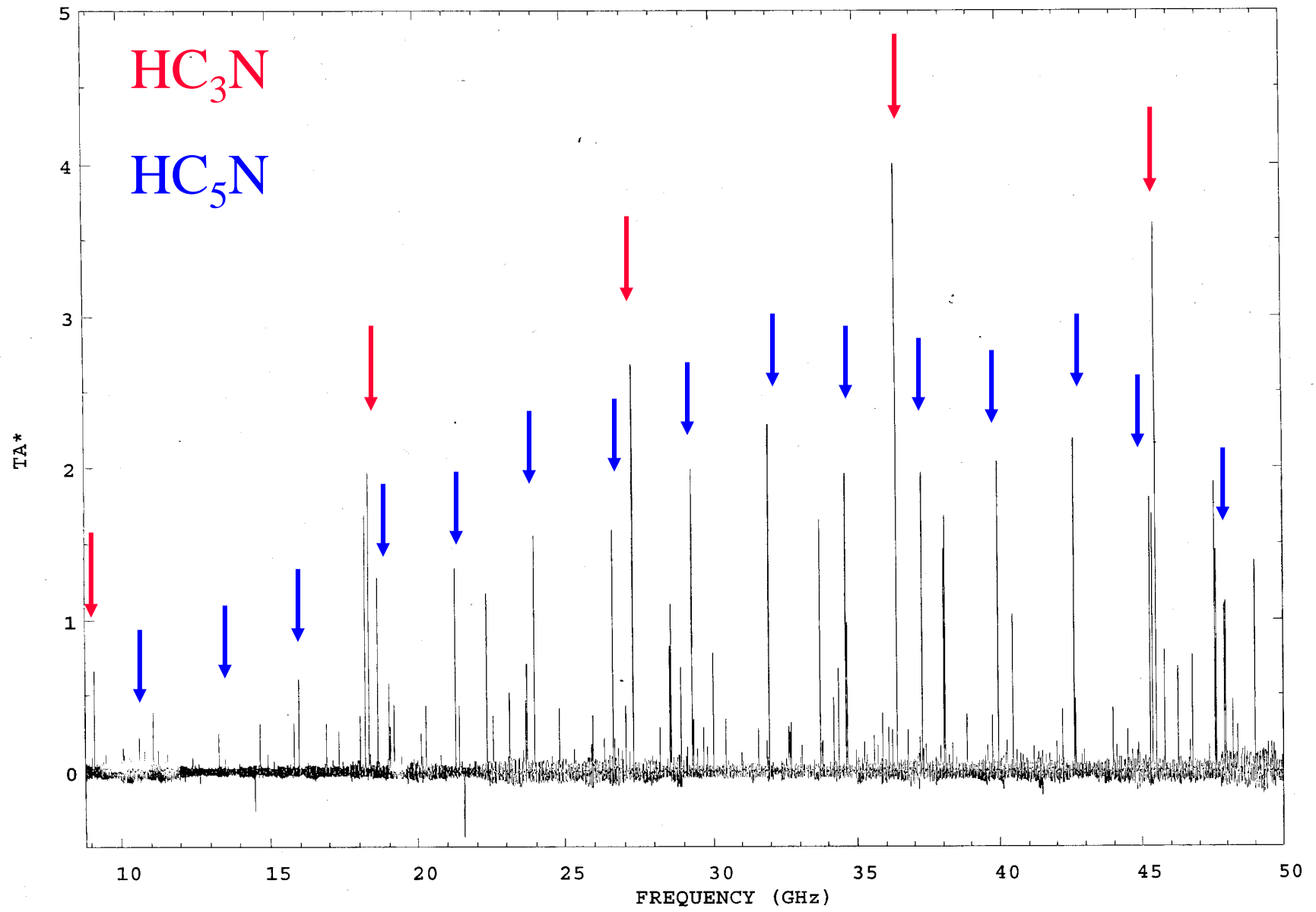
IR: Infrared, Opt: Visible, and UV: Ultraviolet.

* Indicates molecules observed only in Red Giants.

? Reported, however, not yet confirmed.

- Free radicals, ions.
- Carbon chains
- Cyclic molecules





Formation of molecules in interstellar space

- Ion-molecule reactions



- Neutral molecule reactions



- Surface reactions on dust grains



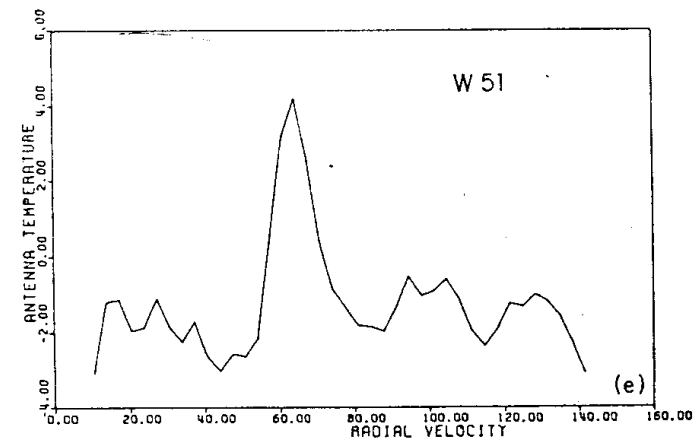
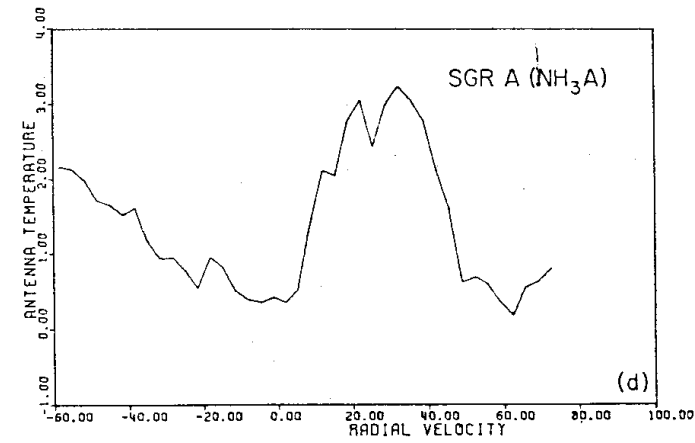
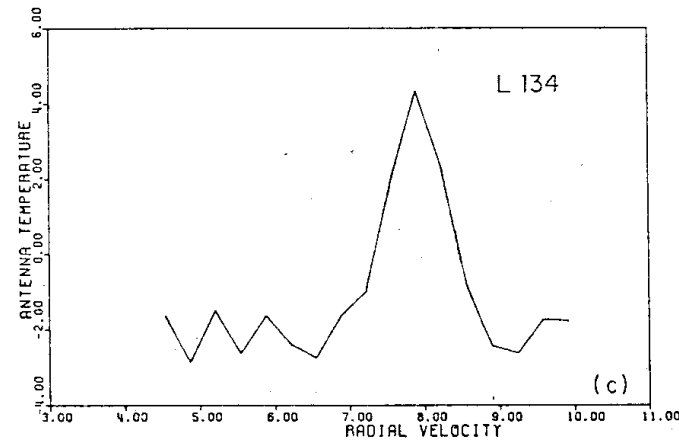
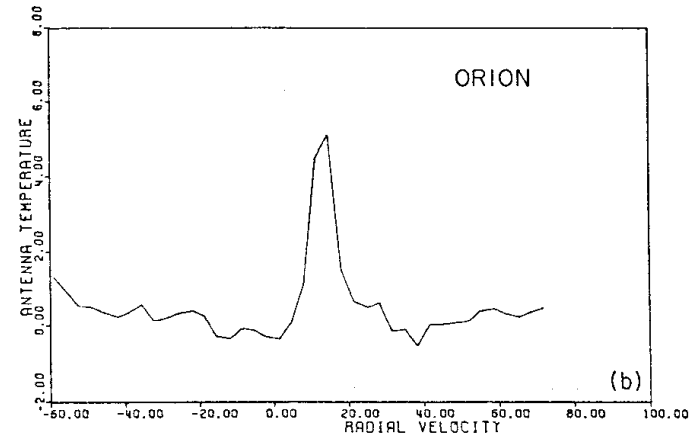
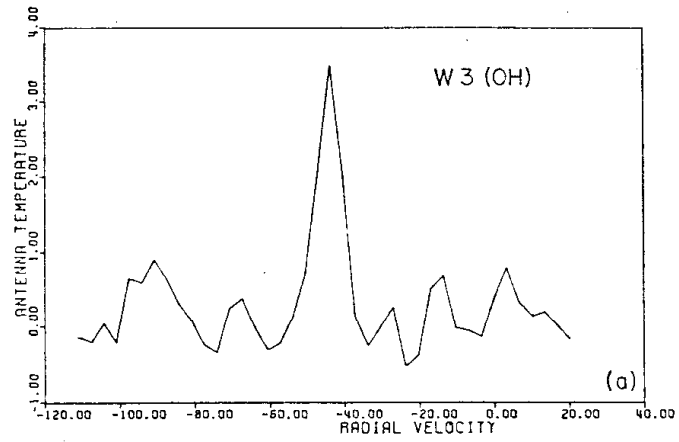
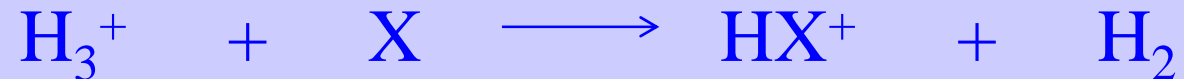
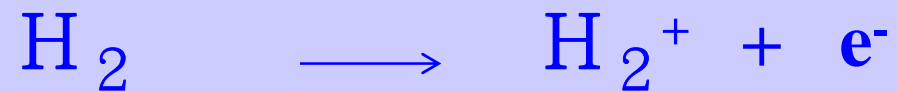


Fig. 1. X-ogen spectra observed for: *a*, W3 (OH); *b*, Orion; *c*, L134; *d*, Sgr A (NH₃A); and *e*, W51. Antenna temperature is in degrees Kelvin uncorrected for antenna efficiency (and dome attenuation in the case of Orion). Radial velocity is in km s⁻¹ corrected to the local standard of rest. Spectrum for L134 taken with 100 kHz filter spacing.

Ion-molecule reaction



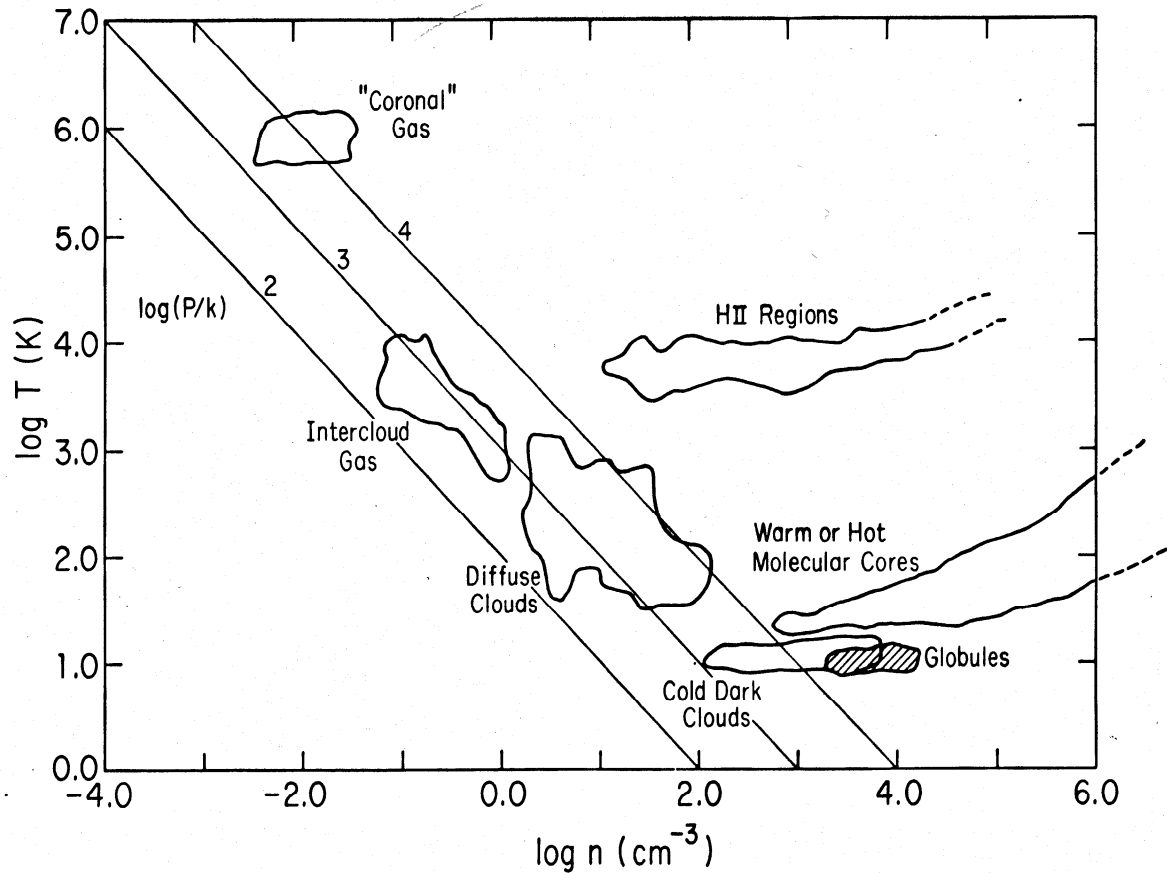


Fig. 4.1. The physical regimes of the interstellar medium, as currently observed.

Particle density of standard atmosphere

$$3 \times 10^{19} / \text{cm}^3$$

Collision interval

$$\sim 10^{-9} \text{ sec}$$

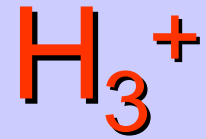
Molecular Clouds

$$10 / \text{cm}^3$$

Collision interval

$$\sim 100 \text{ years}$$

From B. E. Turner



- H_3^+ in the laboratories
- H_3^+ in Jupiter
- H_3^+ in Dark clouds
- H_3^+ in Diffuse clouds
- Dissociative recombination of H_3^+ with electrons

Discovery of H_3^+ spectra

2366

T. Oka

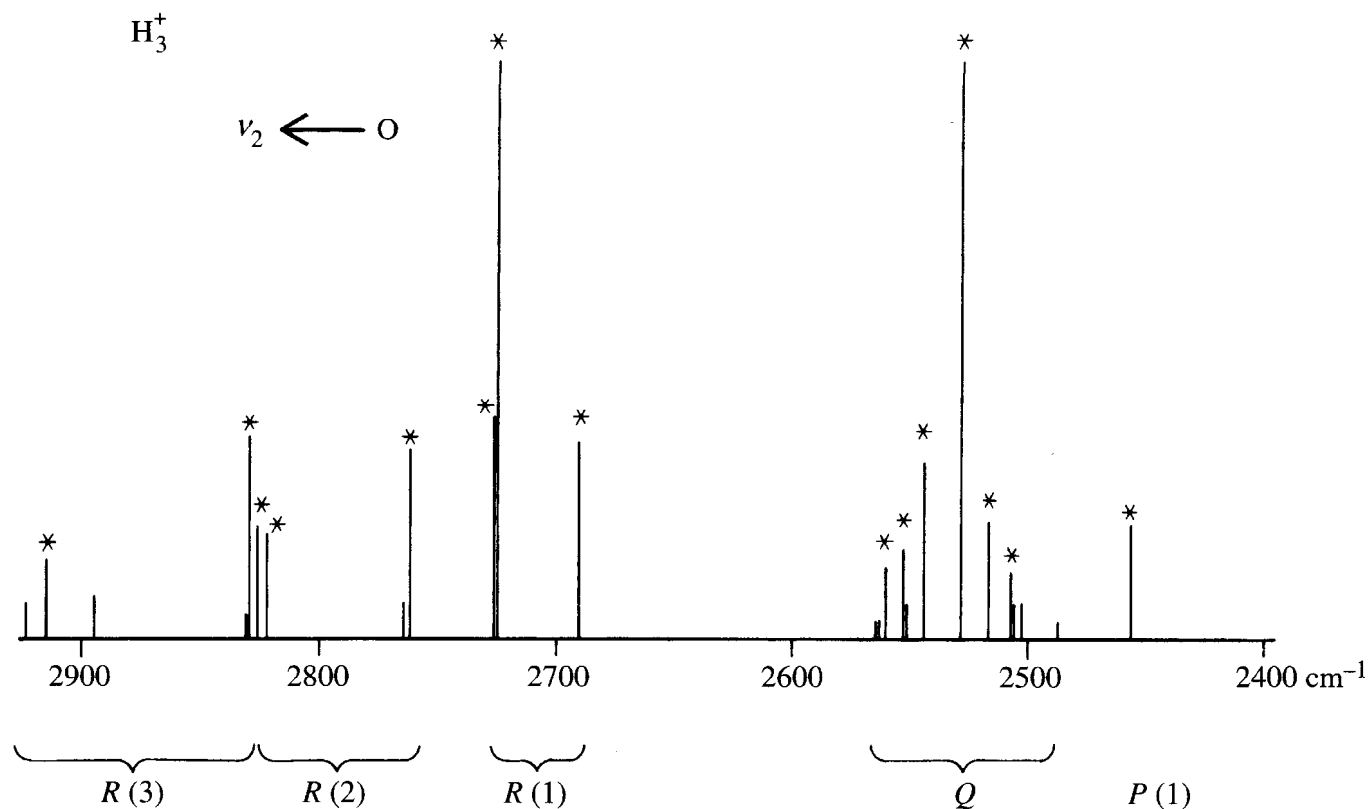


Figure 2. The spectral pattern for the ν_2 band of H_3^+ calculated by Watson for the rotational temperature of 200 K. Observed transitions are marked with asterisks (Oka 1980).

T. Oka, Phys. Rev. Lett. 45, 531-534(1980)

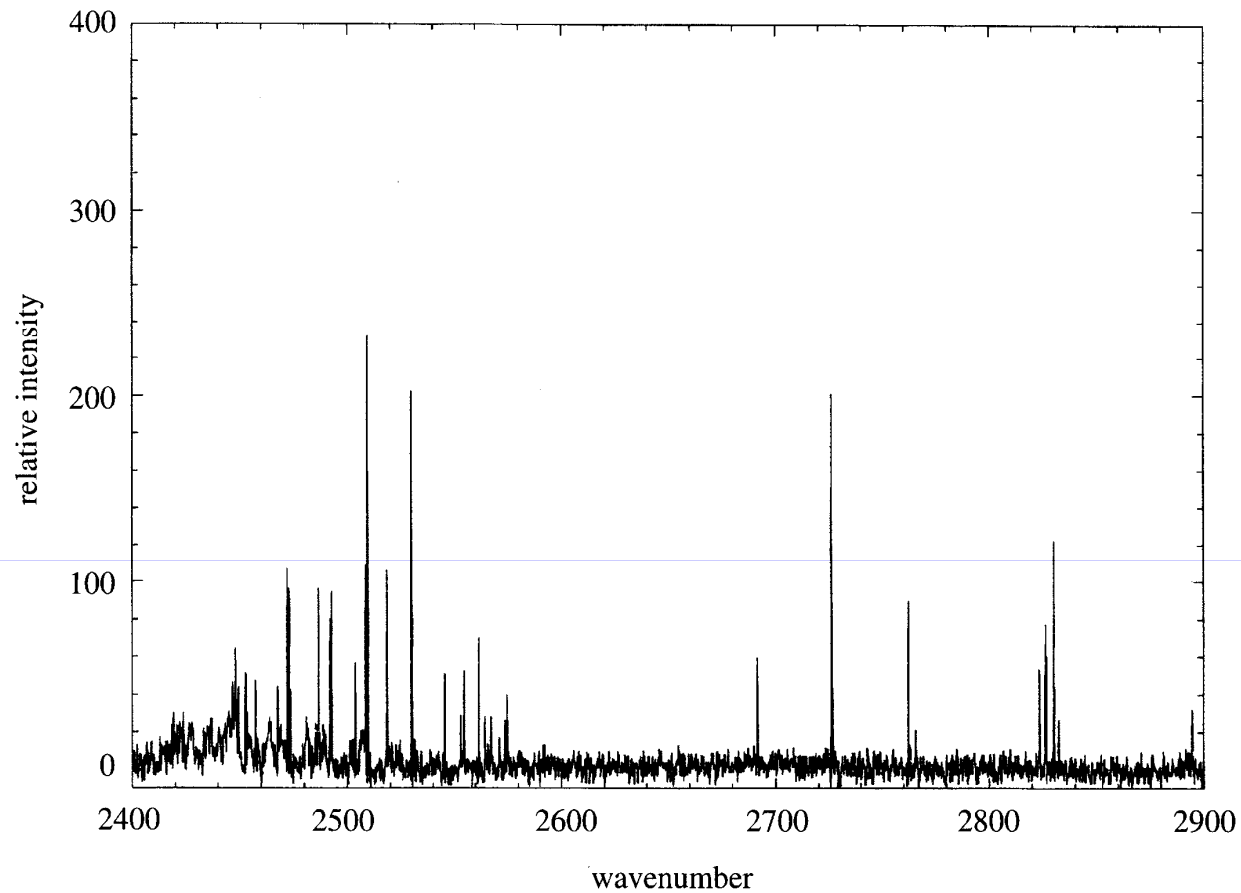
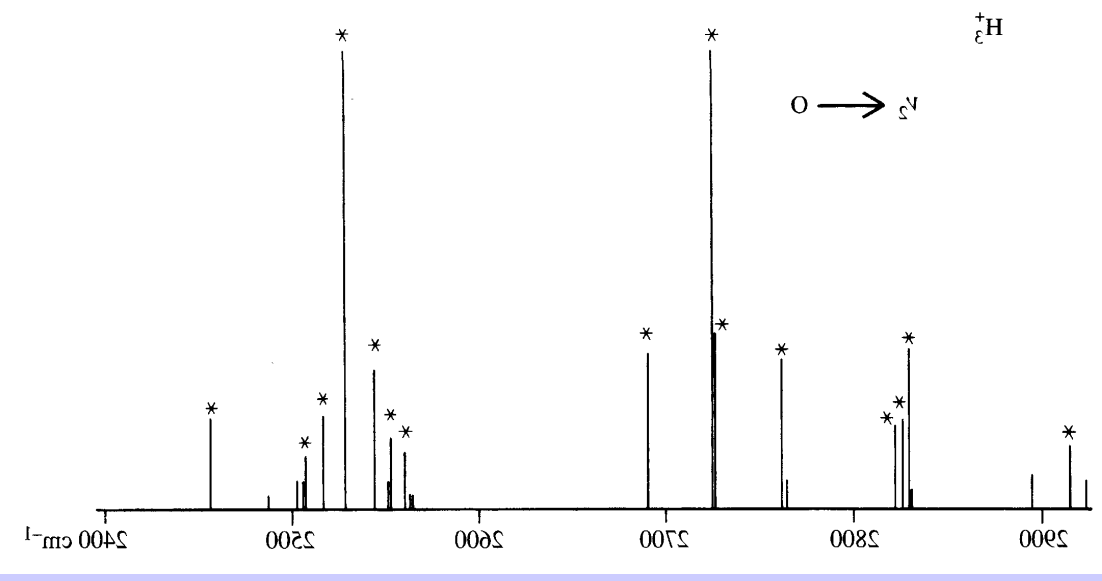
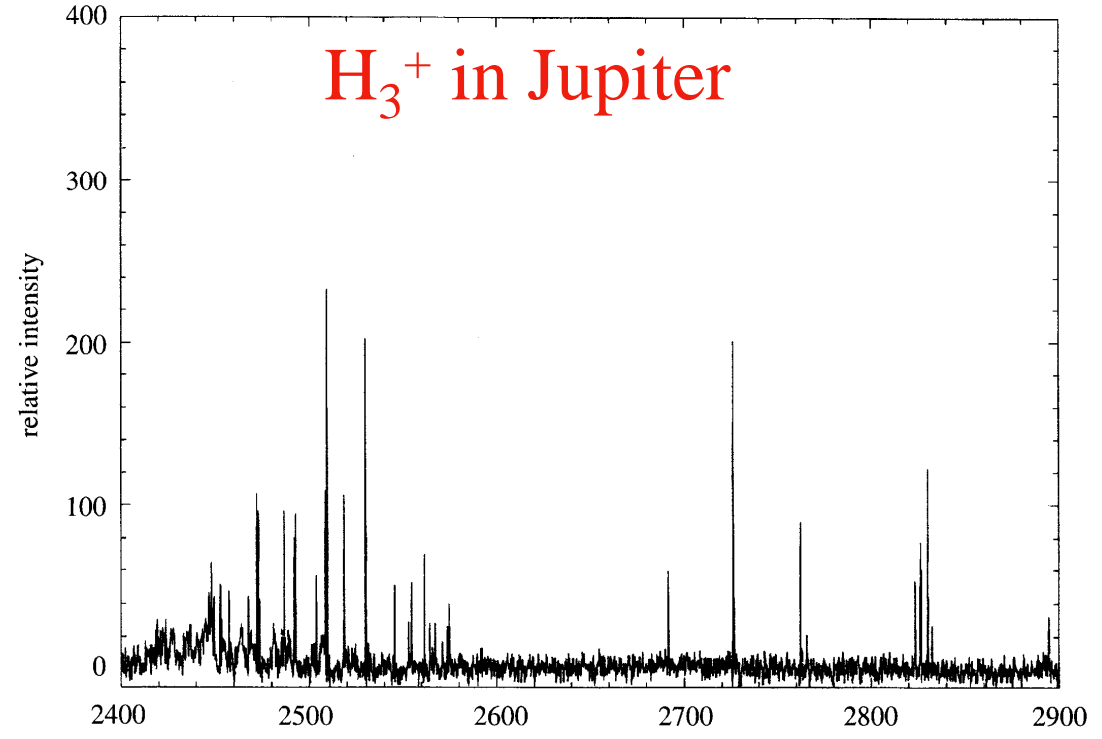


Figure 3. The intense and pure H₃⁺ emission spectrum recorded on the southern hemisphere of Jupiter at 60° latitude and mean longitude 40° (Maillard *et al.* 1990).

J.P. Maillard *et al*, *Astrophys. J.* **363**, L37(1990)



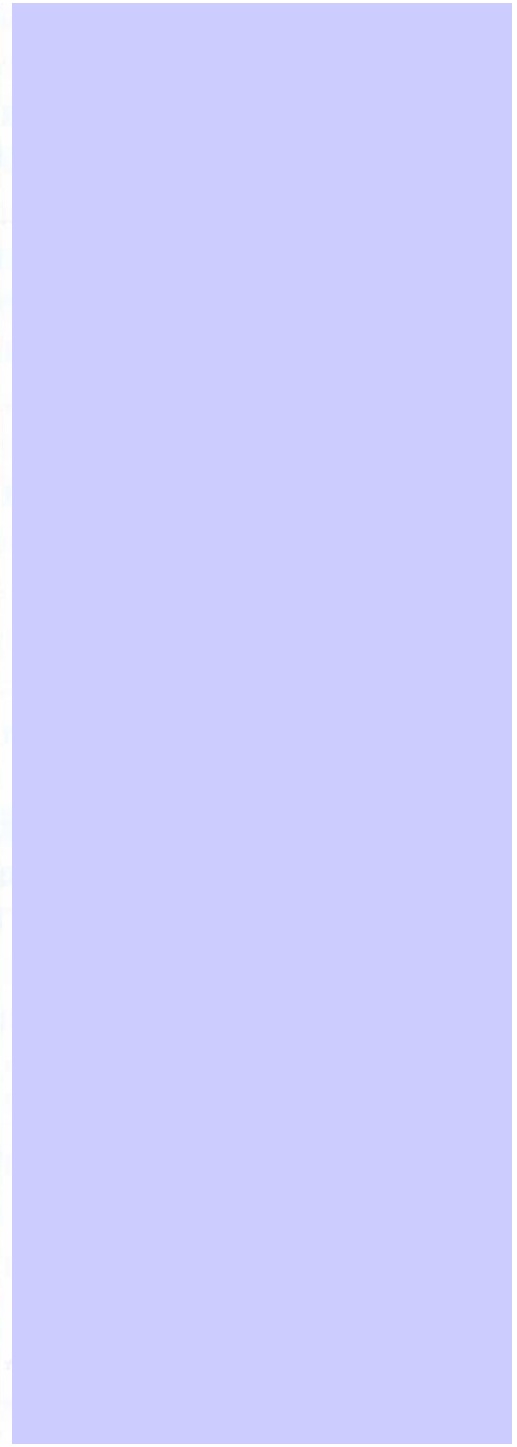
IRTF NSFCAM
29 Jun 1995

Magnetic Equator

Jupiter
89° CML
 $\phi_{Io} = 90^\circ$

$Io - 6 R_j$

$30 R_j$



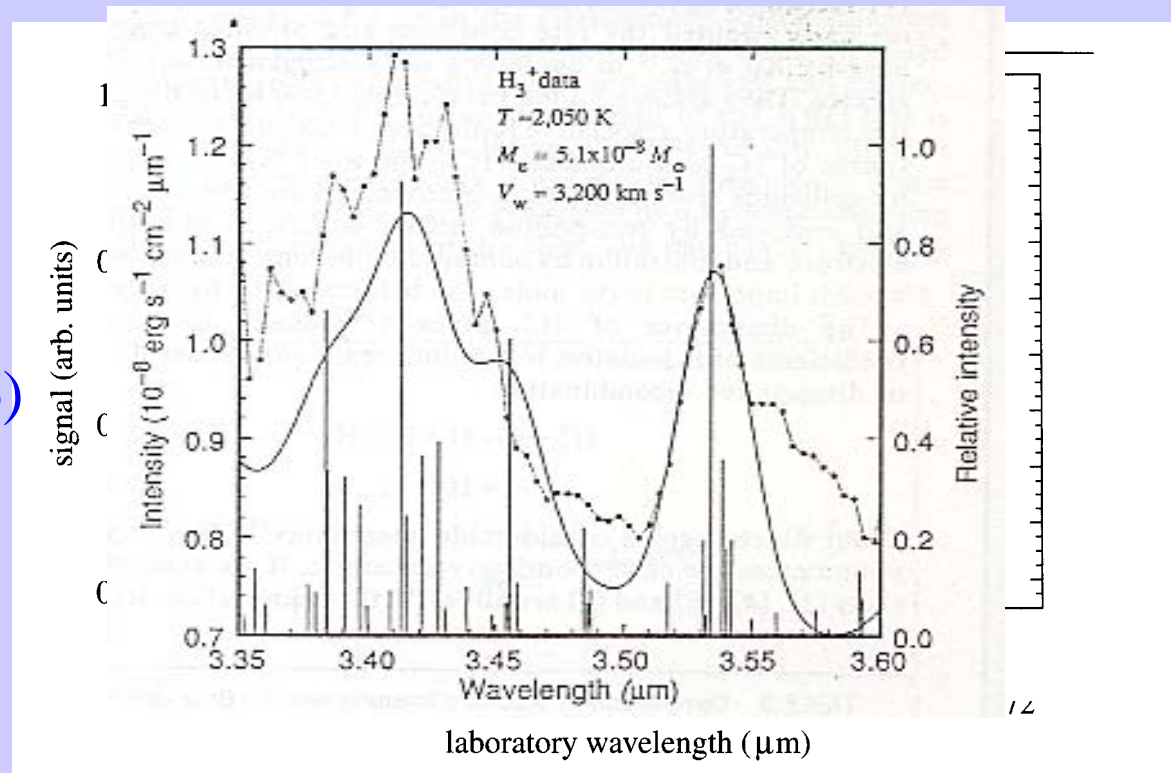
Detection of Interstellar H_3^+

SN1987A Miller, Tennyson, Lepp, and Dalgarno(1992)

Dark cloud

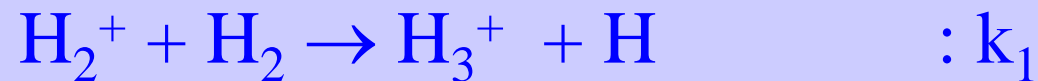
Geballe and Oka(1996)

Diffuse cloud



Geballe, McCall, Hinkle, and Oka(1999)

Formation and destruction of H_3^+



In dark cloud



$$[\text{H}_3^+] \sim \zeta [\text{H}_2] / k_2 [\text{CO}]$$

In diffuse cloud



$$[\text{H}_3^+] \sim \zeta [\text{H}_2] / k_d [e^-]$$

In dark clouds

$$[\text{H}_3^+] \sim \zeta [\text{H}_2] / k_2 [\text{CO}]$$

$$\zeta = 3 \times 10^{-17} \text{ s}^{-1}$$

$$k_2 = 1.8 \times 10^{-9} \text{ cm}^3 \text{ s}^{-1}$$

$$[\text{CO}] / [\text{H}_2] = 1.5 \times 10^{-4}$$

$$[\text{H}_3^+] = 1.1 \times 10^{-4} \text{ cm}^{-3}$$

Observed Column densities

$$[\text{H}_3^+]L = 6 \times 10^{14} \text{ cm}^{-2} \quad \text{W33}$$

$$= 4 \times 10^{14} \text{ cm}^{-2} \quad \text{GL2136} \Rightarrow L = 1 \sim 2 \text{ pc}$$

In diffuse clouds

$$[\text{H}_3^+] \sim \zeta [\text{H}_2] / k_d [\text{e}^-]$$

$$\zeta = 3 \times 10^{-17} \text{ s}^{-1}$$

$$k_d = 1.8 \times 10^{-7} \text{ cm}^3 \text{ s}^{-1} \quad (4.6 \times 10^{-7})$$

$$[\text{e}^-] / [\text{H}_2] = 5.6 \times 10^{-4}$$

$$[\text{H}_3^+] = 1.1 \times 10^{-7} \text{ cm}^{-3}$$

Observed Column density

$$[\text{H}_3^+]L = 3.8 \times 10^{14} \text{ cm}^{-2} \quad \text{Cyg OB2 No.12}$$

$$\Rightarrow L = 400 \sim 1200 \text{ pc}$$

High-resolution Spectroscopy of Negative ions

- OH⁻ (OD⁻)

IR, FIR

- SH⁻ (SD⁻)

IR, sub-mm

- FHF⁻, ClHCl⁻, NH₂⁻, NCO⁻, NCS⁻, N₃⁻

IR

Mystery of “B1377”

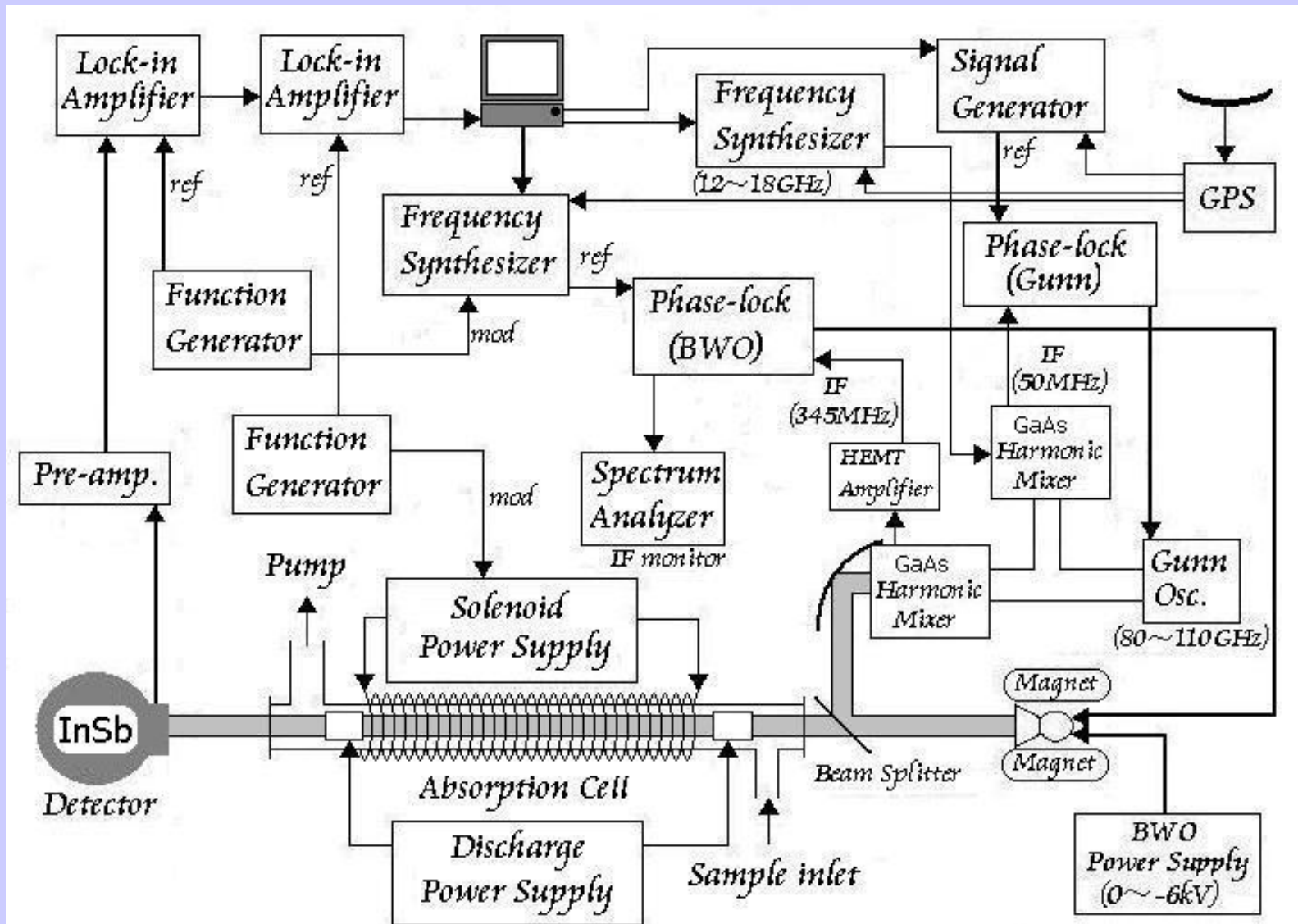
- Kawaguchi et al (1995)
Detected a series of emission lines toward IRC+10216.
Linear molecule of the rotational constant of
1376.86868 MHz.
- Aoki (2000)
“Carrier of B1377 is very likely to be C_6H^- .”
- McCarthy et al (2006)
Succeeded in the laboratory detection of B1377, and in
astronomical detection in TMC-1.

 C_5N^- (Cernicharo *et al*, 2008)

Waterloo sub-mm system

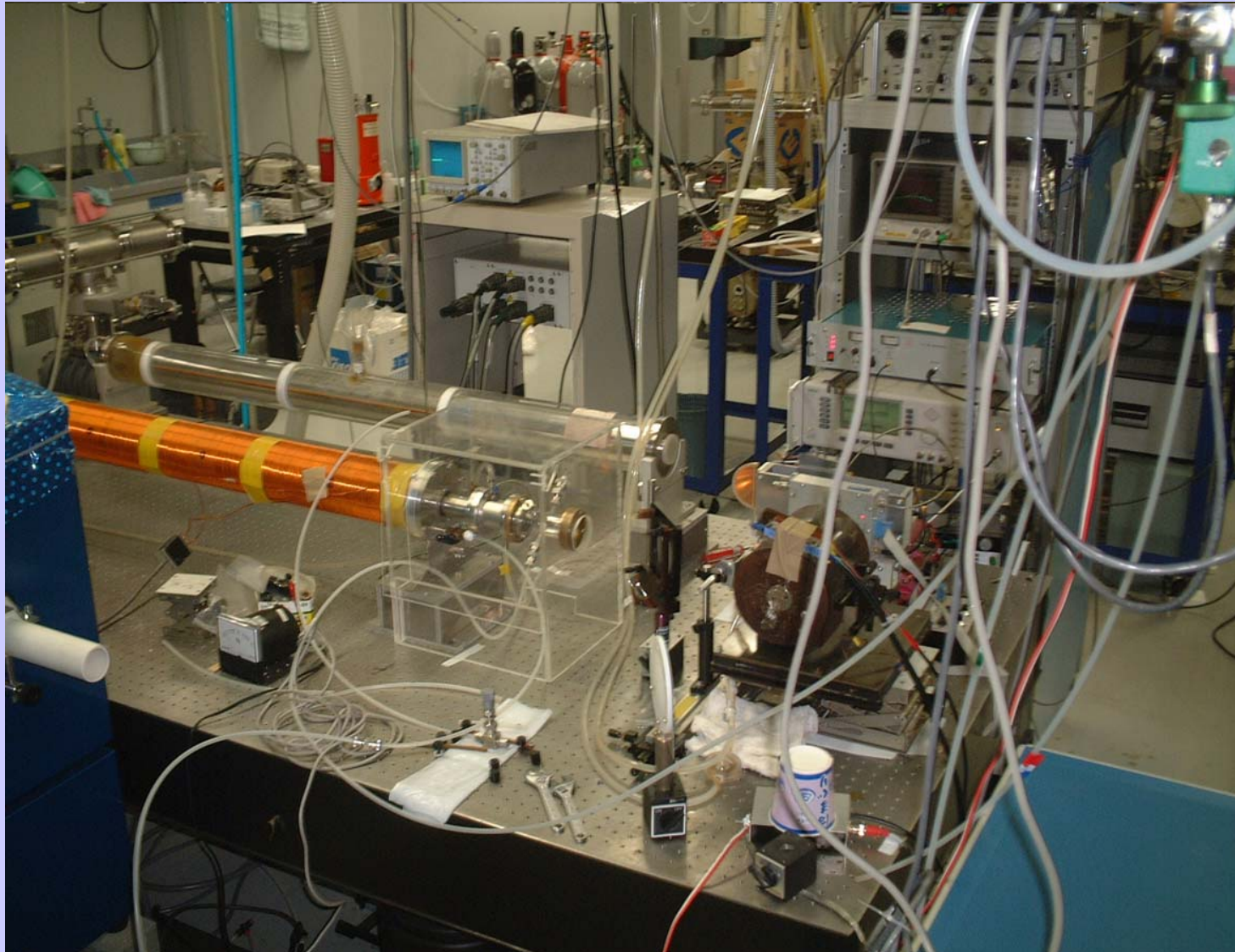
- The frequency range of 270-890 GHz is covered with four BWOs (Backward-wave oscillator) with ~ 1 mW power.
- The absorption cell is designed to detect positive ions.
- Mostly operated in extended negative glow discharge mode with longitudinal magnetic field of ~ 250 Gauss.

Double modulation sub-mm system at Waterloo



Submillimeter-wave system in Ibaraki

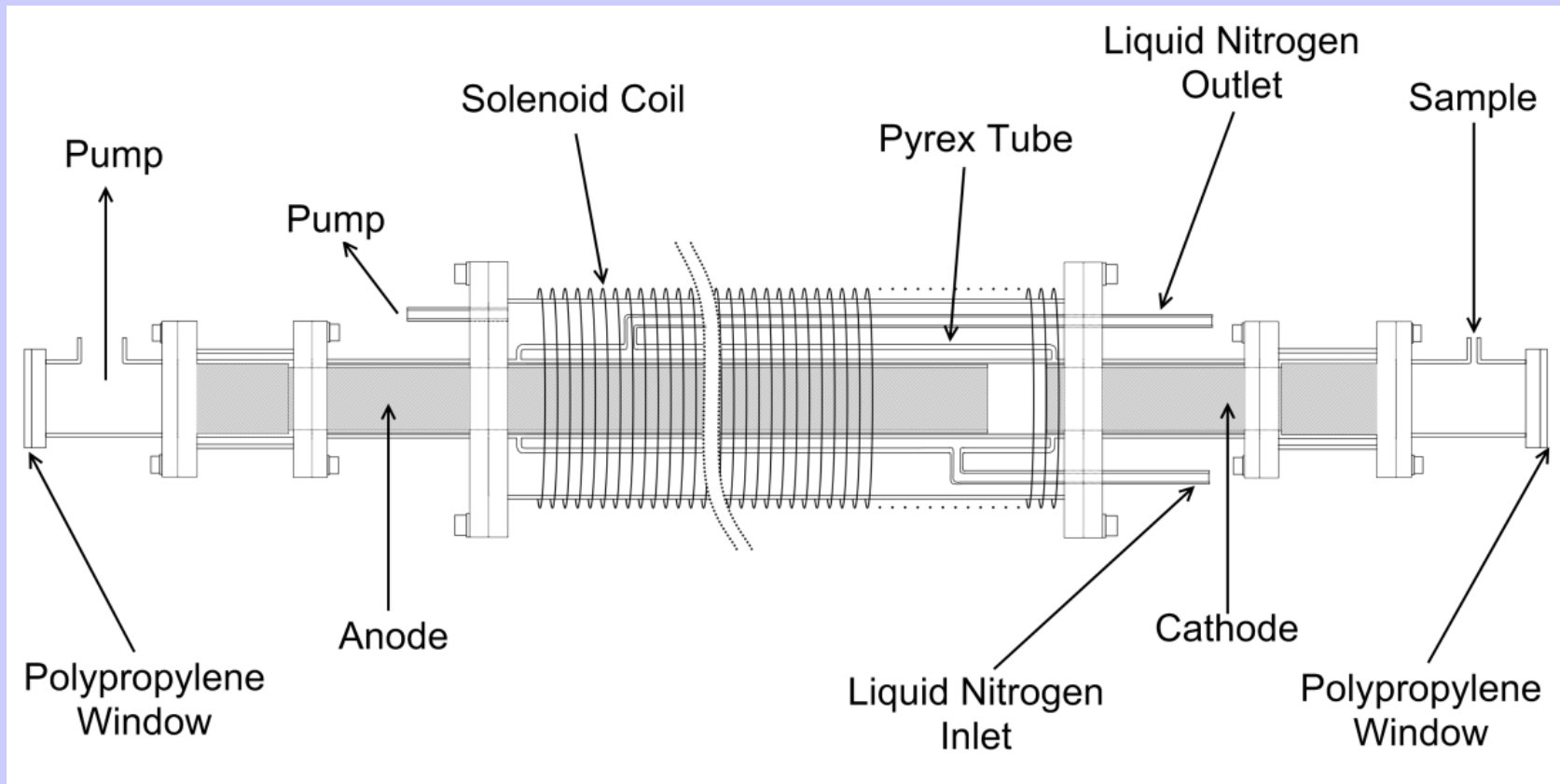
Now moved to Waterloo



Three types of discharges are tried for detection of anions

- Glow discharge
- Hollow anode discharge
- Extended negative glow discharge

Hollow-anode cell



↔

7 cm

↔

1.6 m

↔

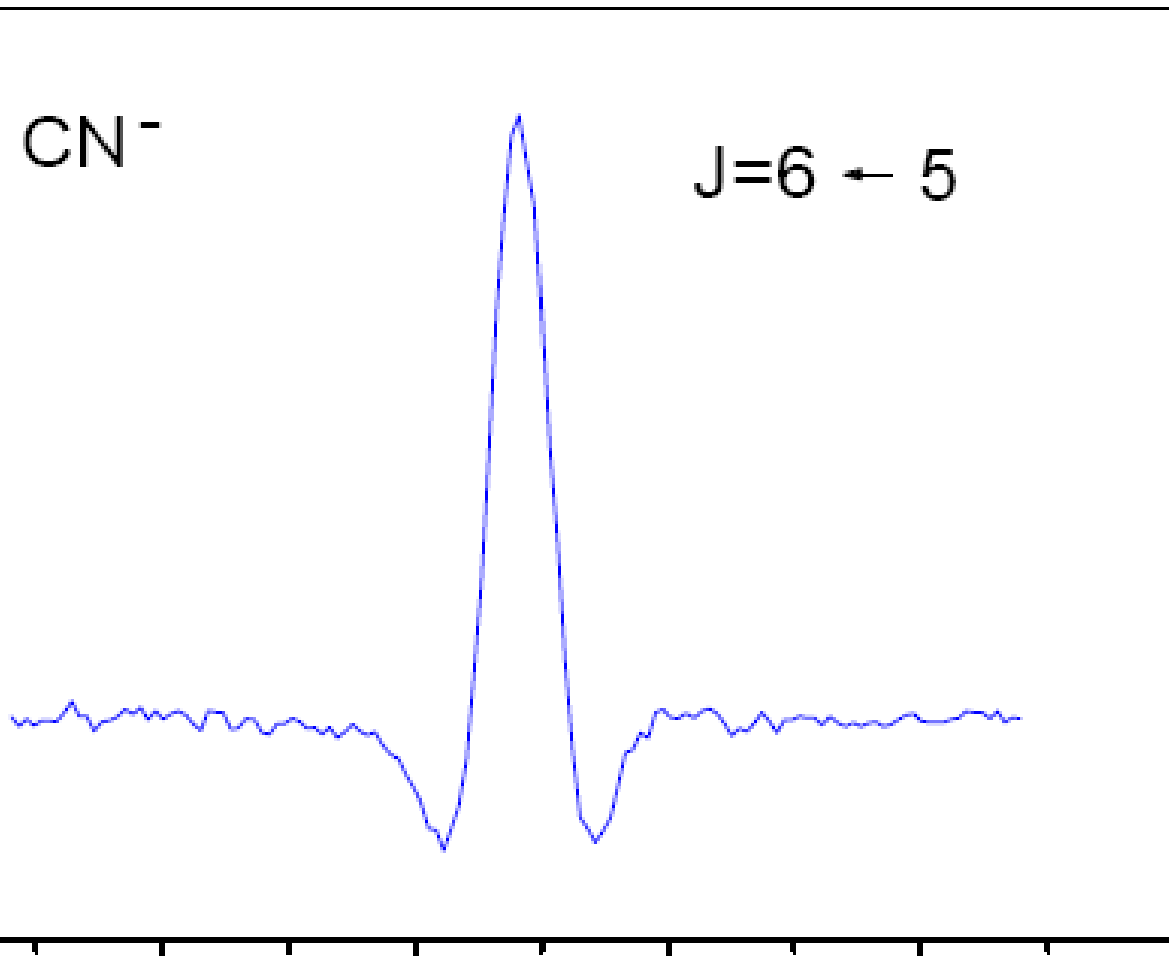
1.8 m

CN⁻

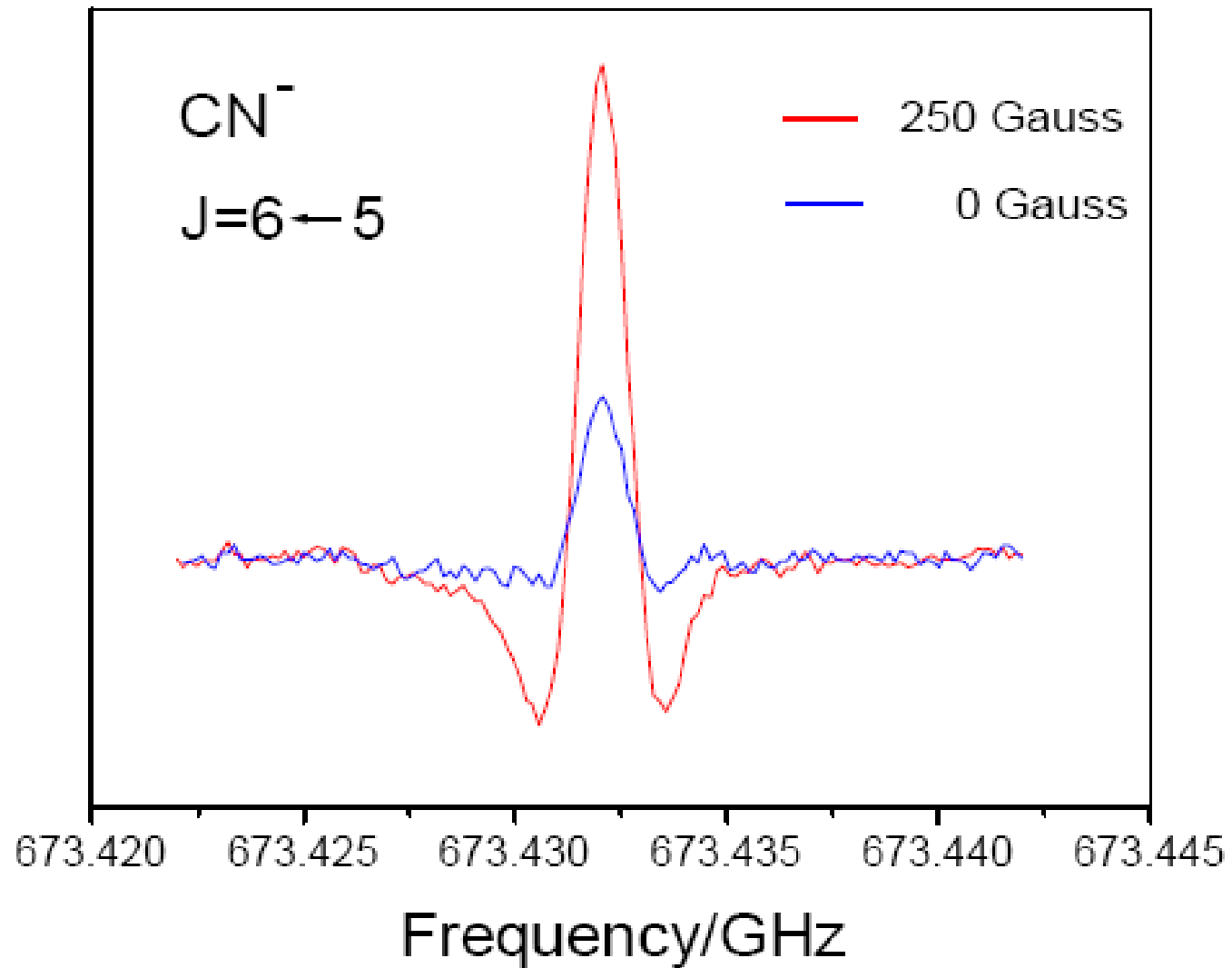
J=6 ← 5

673.420 673.425 673.430 673.435 673.440 673.445

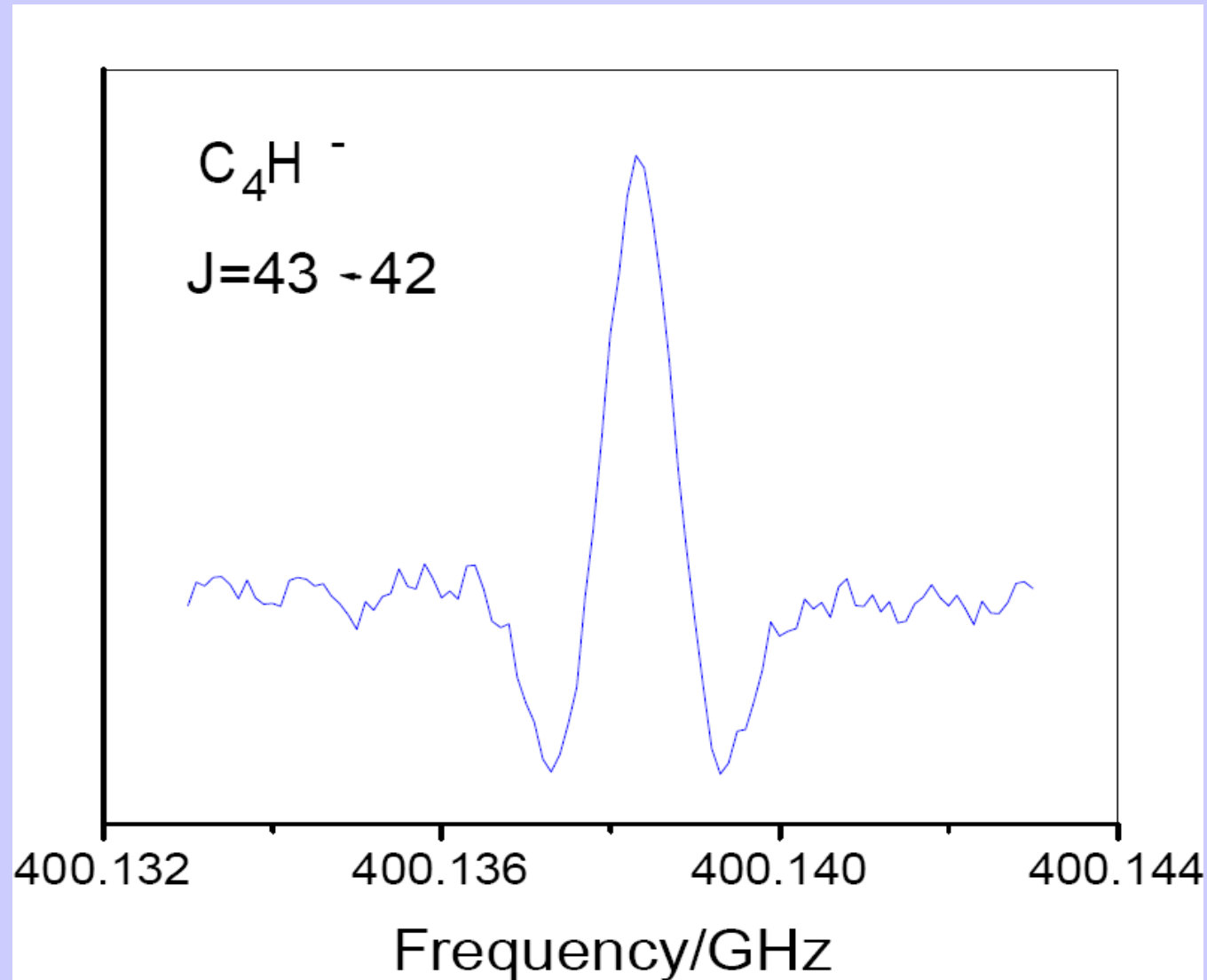
Frequency/GHz



CN⁻ in “hollow anode” discharge



C_4H^- in extended negative glow discharge

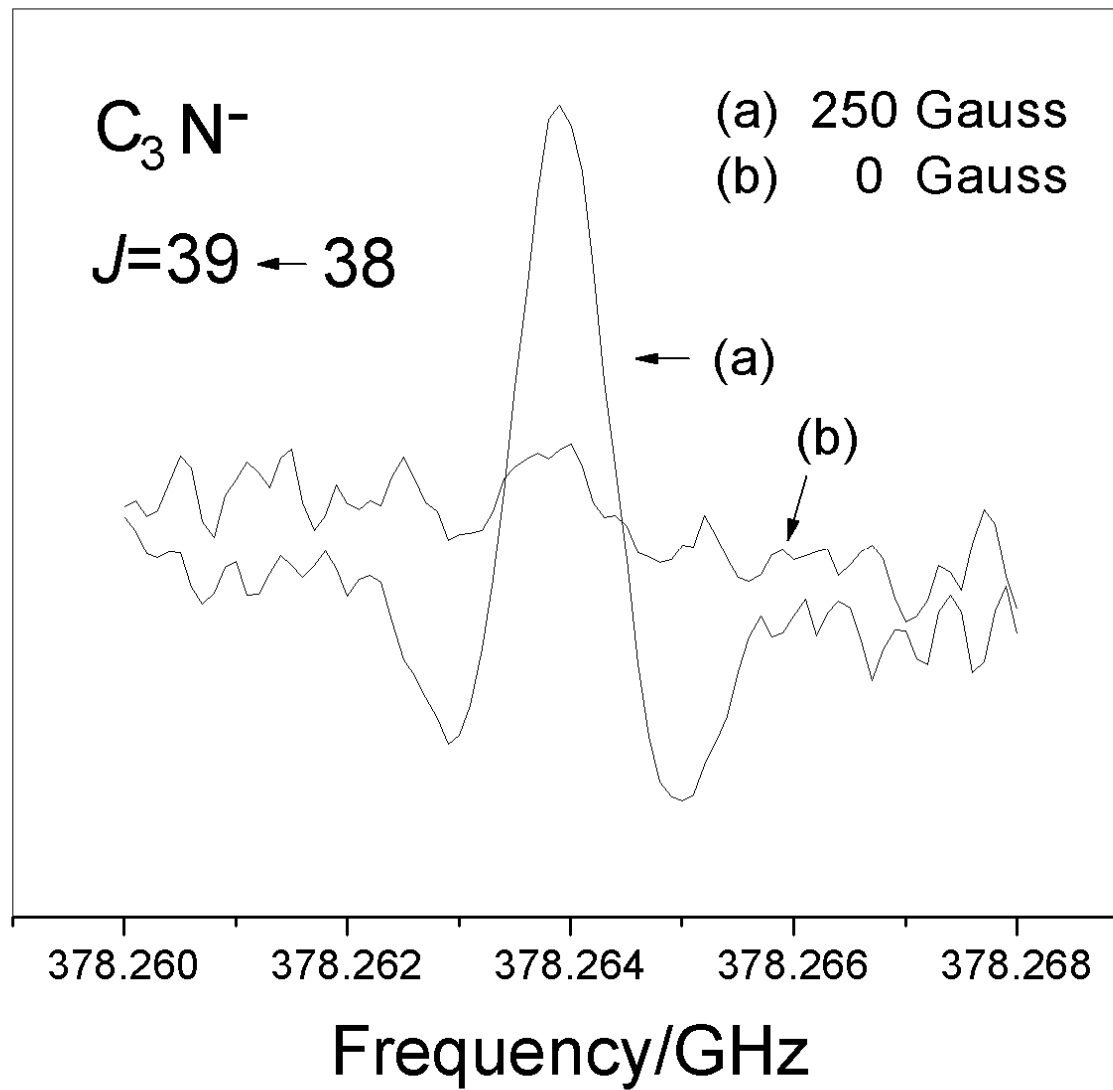


Sub-mm observations of C_3N^-

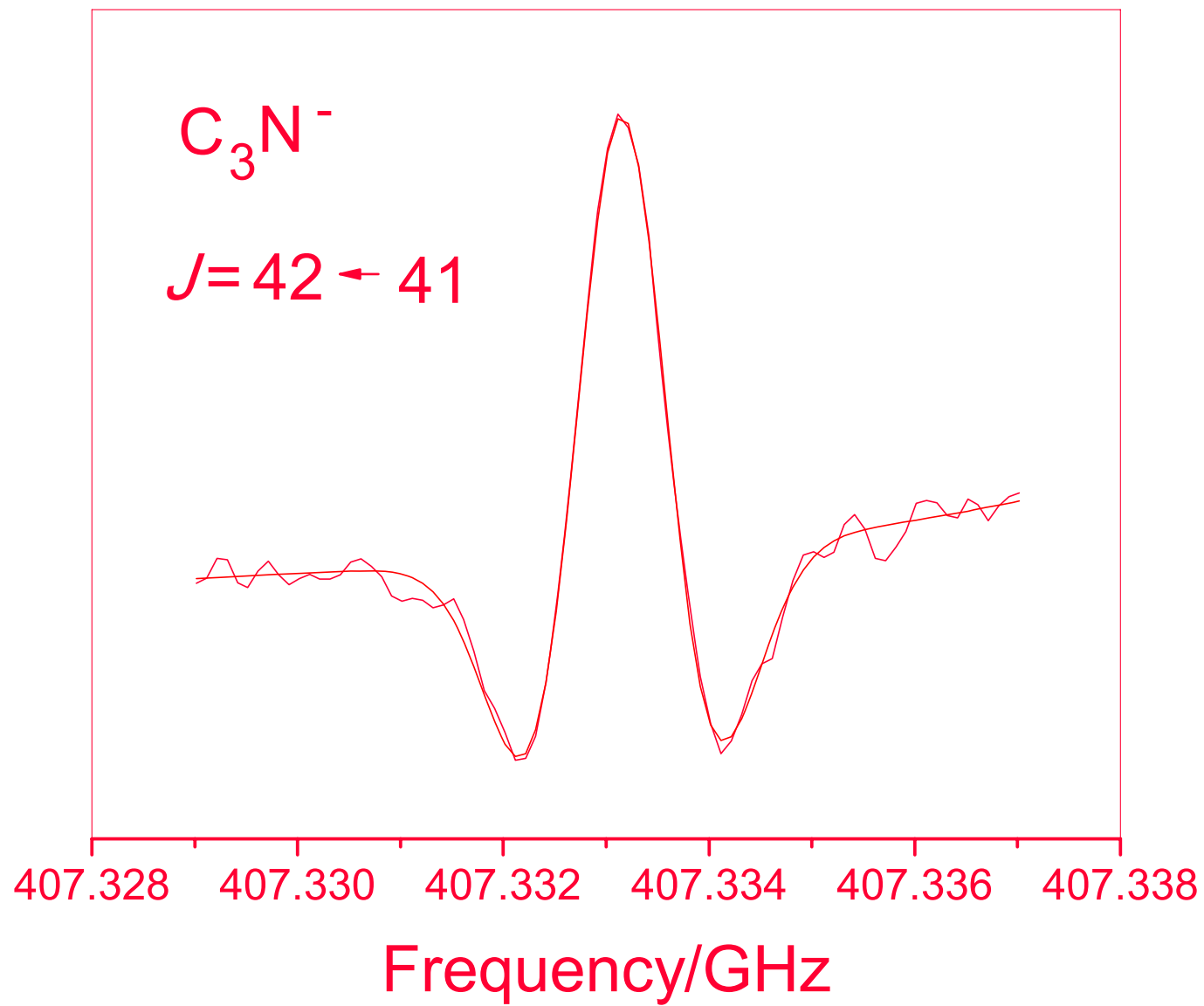
- Production ;
 $C_2N_2 \leq 1$ mTorr + $C_2H_2 \sim 2$ mTorr + Ar 12 mTorr
in either
“hollow anode discharge” or
extended negative glow discharge
of 4~10 mA, cooled to 210 K.
Freq. range ~ 504 GHz

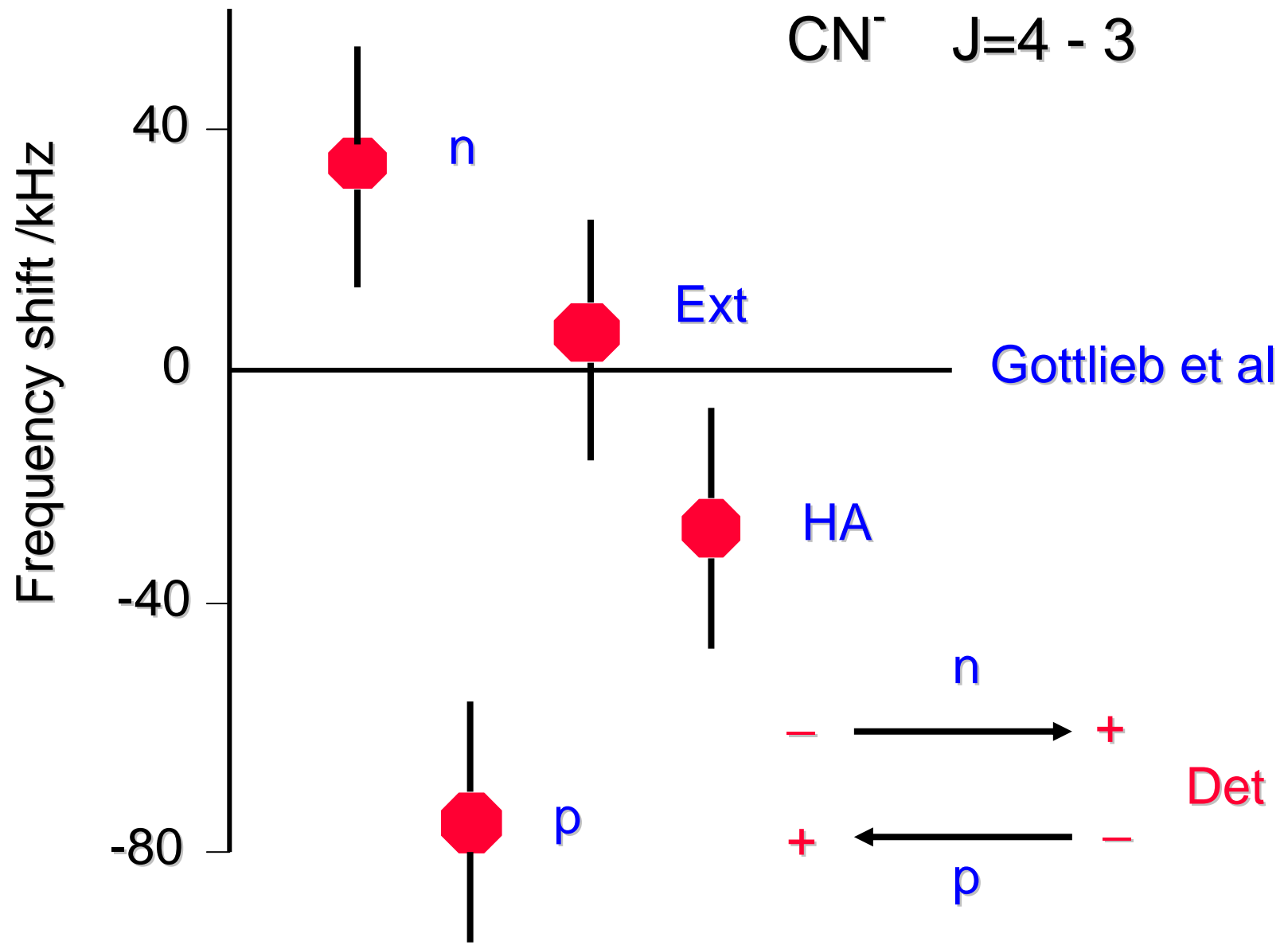
Thaddeus et al, HC_3N (20 %) + Ar (80 %) ~ 15 mTorr
dc discharge current of 20 mA at 200 K.

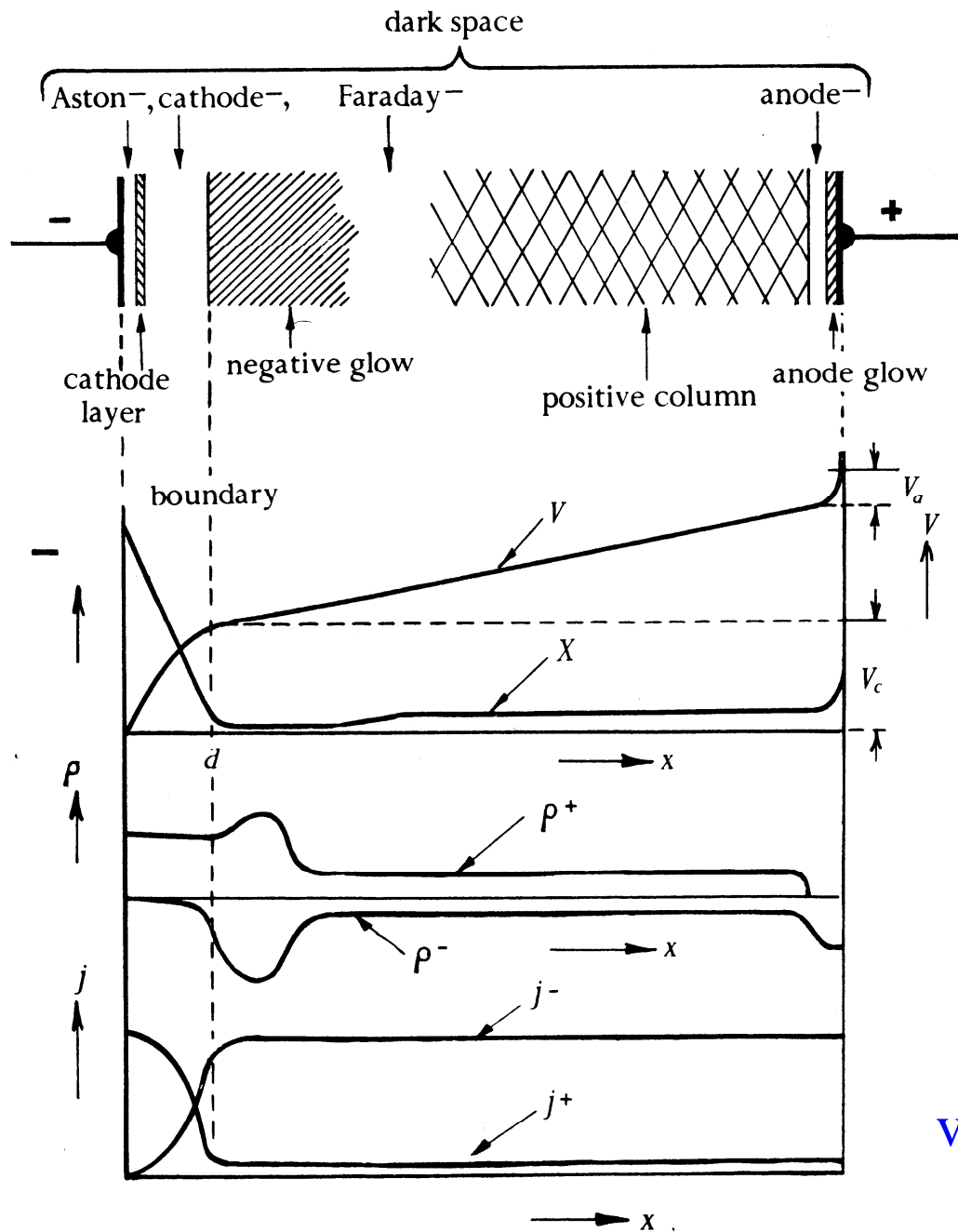
Extended Negative Glow



Hollow-anode discharge







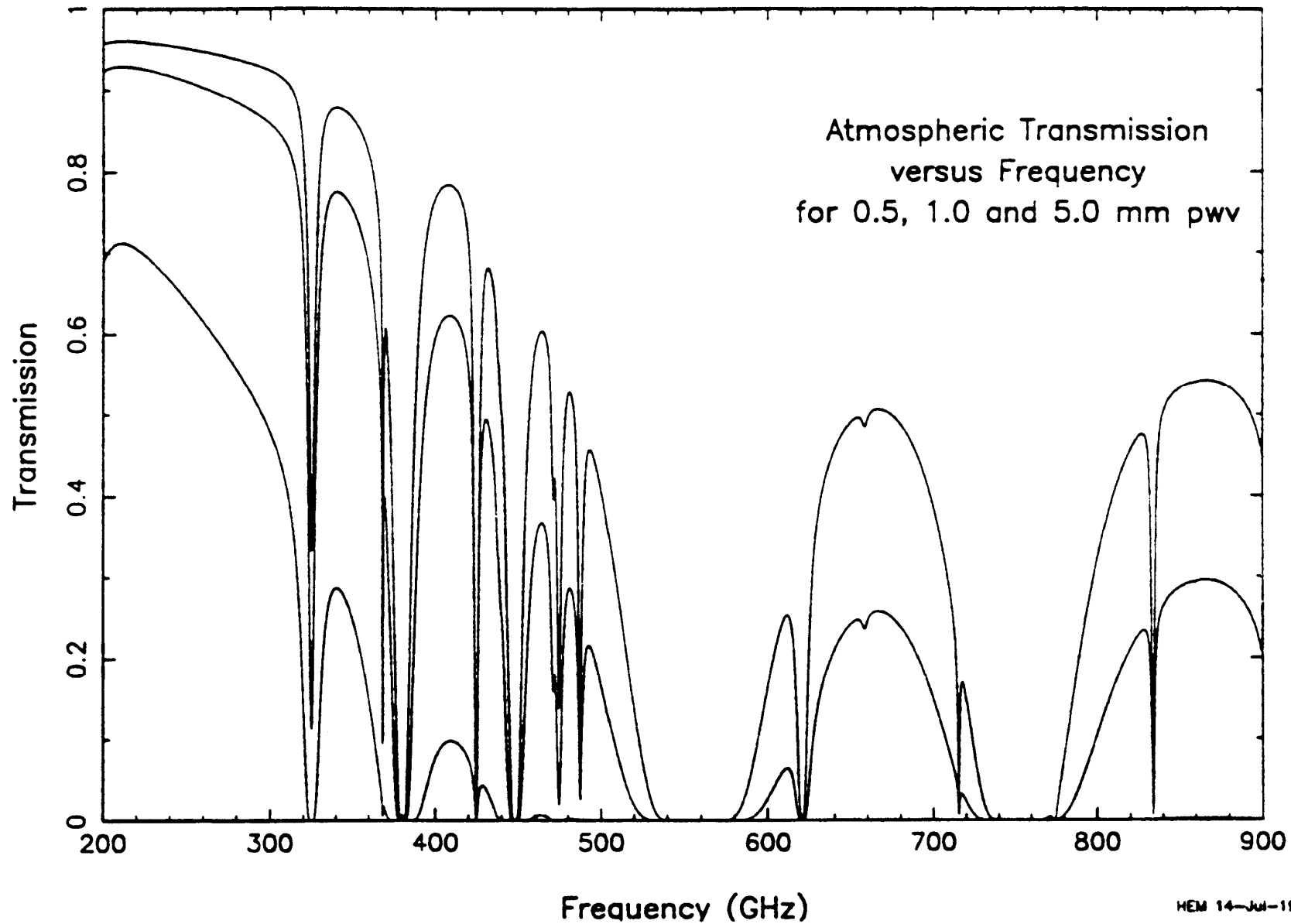
Density of negative charges is high in negative glow and anode glow

von Engel "Ionized Gases"

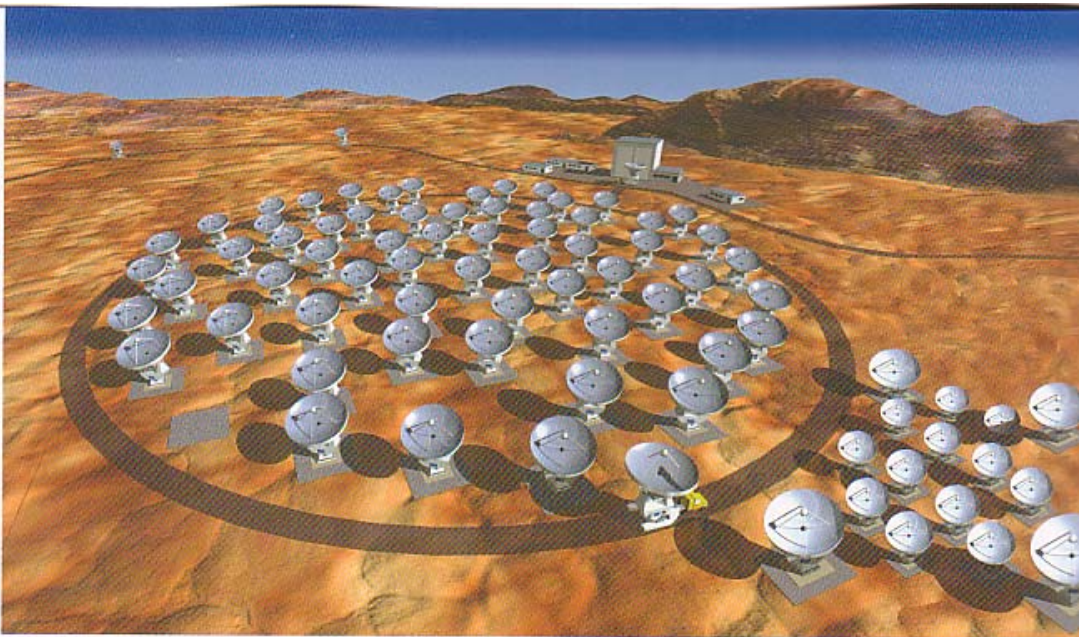
Why sub-mm now?

- Ground- and satellite-based astronomical and/or atmospheric observation platforms.
 - Higher spatial resolution with shorter wavelength.
 - Better sensitivity.
- Easy to use laboratory system.
 - multipliers.
 - BWOs.

Atmospheric Opacity in the submillimeter-wave region



Original CG courtesy of ESO,
modified by NAOJ

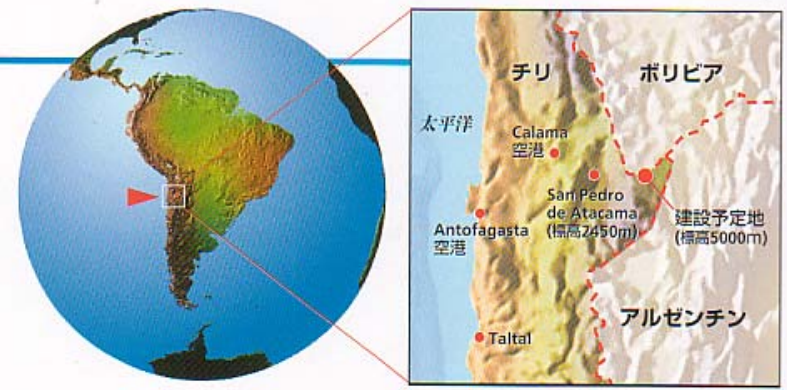


7)

ALMAは、日本・北アメリカ・ヨーロッパの諸国が協力して、チリ・アンデス山中の標高5000mの高原に建設することを計画している、アタカマ大型ミリ波サブミリ波干渉計 (**Atacama Large Millimeter/submillimeter Array**) の略称です。直径12mの高精度アンテナ64台と「ACAシステム」と呼ばれる超高精度アンテナ16台からなる、全部で80台のアンテナを干渉計方式で組み合わせ、ひとつの巨大な電波望遠鏡を合成します。電波の中で最も波長が短く、最高の周波数帯である「ミリ波・サブミリ波」を使って、ビッグバン後間もない宇宙初期における銀河の誕生、今も続くさまざまな惑星系の誕生、そして生命につながる物質の進化を解き明かします。

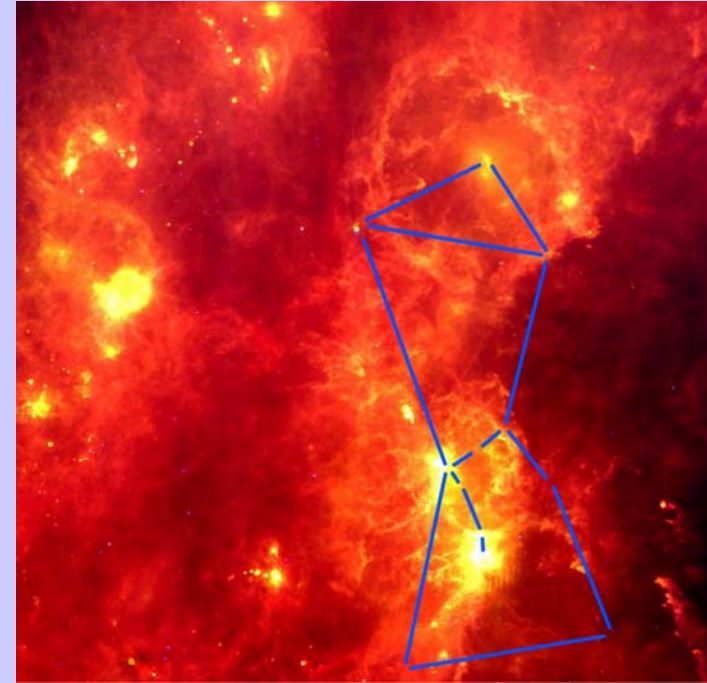
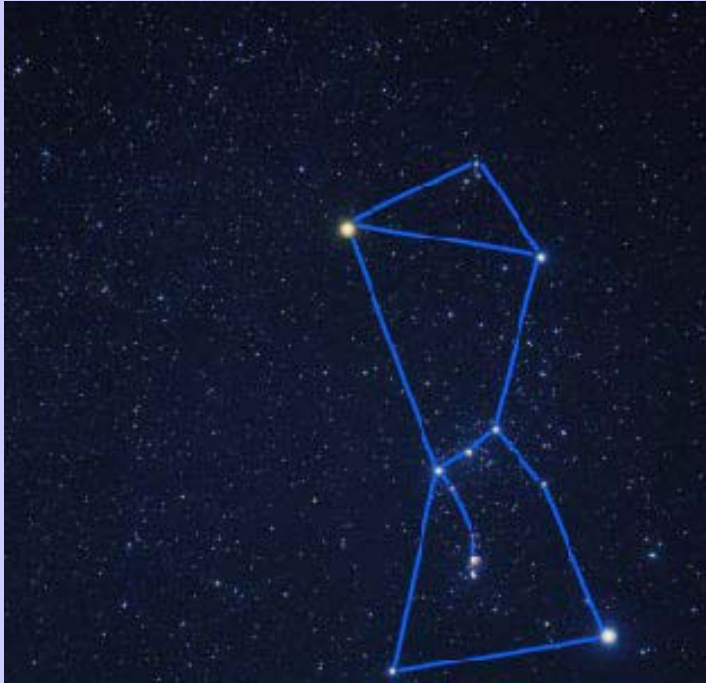
宇宙に一番近い場所

ALMAの設置場所は、チリ共和国北部にあるアタカマ砂漠に近い、アンデス山中の標高約5000mの高原です。世界の候補地を詳しく調査・比較した結果、乾燥した気候、高い標高、平坦な地形、そして安全で容易なアクセスという条件を満たす、この土地が選ばれました。



Getting the WHOLE picture

- ◆ An object can look radically different depending on the type of light collected from it:

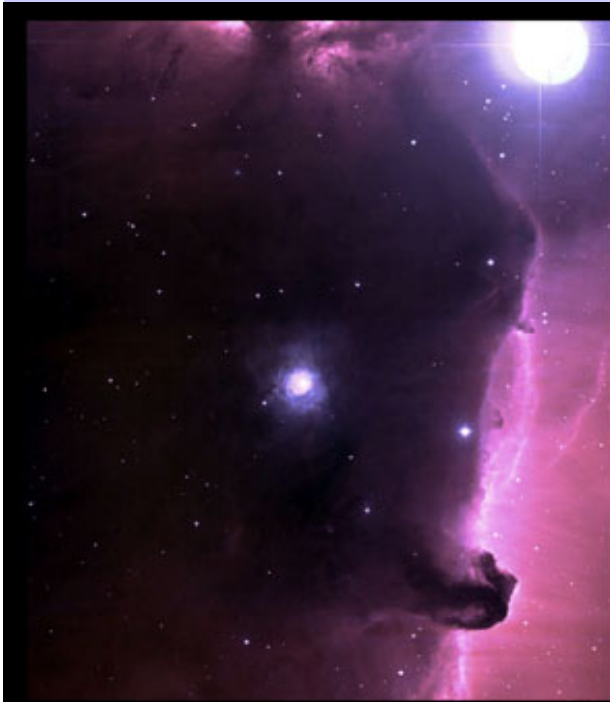


Constellation Orion
left: visual wavelengths
right: far-infrared image

From NASA
web page

- Visible: dark nebula, heavily obscured by interstellar dust
- Near-IR: dust is transparent, embedded proto-stars can be observed
- Mid- and far-IR: glow from cold dust is directly observable

From NASA web page



Visible



Near Infrared



Mid-Infrared



NASA/DLR

A RIGOROUS ATTEMPT TO VERIFY INTERSTELLAR GLYCINE

L. E. SNYDER,¹ F. J. LOVAS,² J. M. HOLLIS,³ D. N. FRIEDEL,¹ P. R. JEWELL,⁴ A. REMIJAN,^{1,3,5}
V. V. ILYUSHIN,⁶ E. A. ALEKSEEV,⁶ AND S. F. DYUBKO⁶

Received 2004 May 25; accepted 2004 October 7

ABSTRACT

In 2003, Kuan and coworkers reported the detection of interstellar glycine ($\text{NH}_2\text{CH}_2\text{COOH}$) based on observations of 27 lines in 19 different spectral bands in one or more of the sources Sgr B2(N-LMH), Orion KL, and W51 e1/e2. They supported their detection report with rotational temperature diagrams for all three sources. In this paper we present essential criteria that can be used in a straightforward analysis technique to confirm the identity of an interstellar asymmetric rotor such as glycine. We use new laboratory measurements of glycine as a basis for applying this analysis technique, both to our previously unpublished 12 m telescope data and to the previously published Swedish-ESO Submillimetre Telescope (SEST) data of Nummelin and colleagues. We conclude that key lines necessary for an interstellar glycine identification have not yet been found. We identify some common molecular candidates that should be examined further as more likely carriers of several of the lines reported as glycine. Finally, we illustrate that a rotational temperature diagram used without the support of correct spectroscopic assignments is not a reliable tool for the identification of interstellar molecules.

Subject headings: ISM: abundances — ISM: clouds —

ISM: individual (Sagittarius B2(N-LMH), Orion Kleinmann-Low, W51 e1/e2) —

ISM: molecules — radio lines: ISM

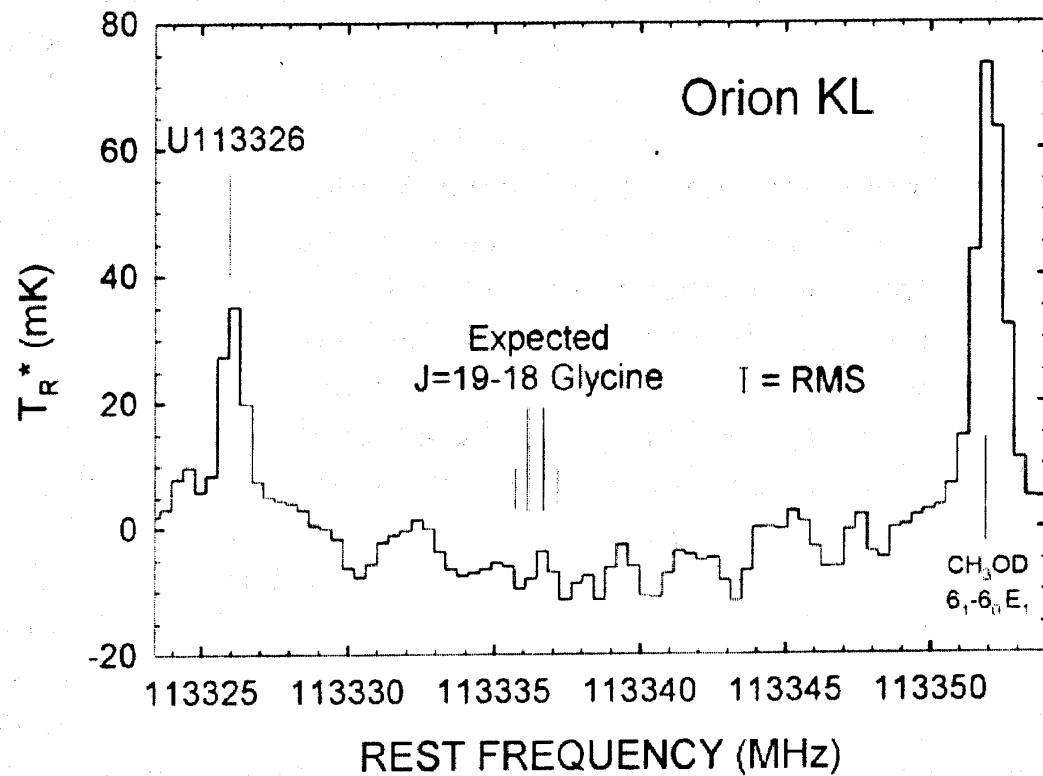
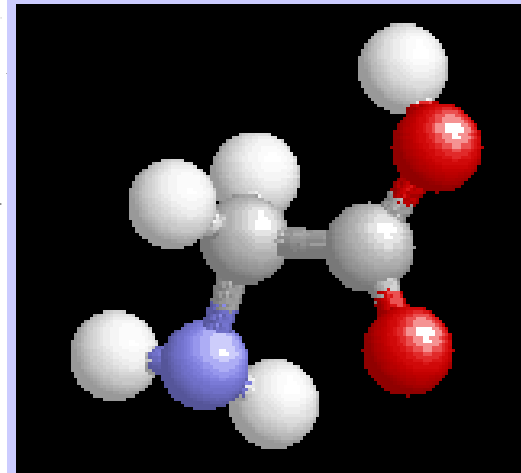


FIG. 1.—Orion KL spectra from 113323 to 113355 MHz (centered at 113339 MHz) observed with the hybrid spectrometer on the NRAO 12 m telescope. The spectral positions of the negative results for the nearly fourfold degenerate $J = 19-18$ glycine lines are marked by the four vertical lines centered at 113336 MHz. U113326 is on the left, and CH_3OD is on the right. The ordinate is in units of mK on the T_R^* scale. The abscissa is rest frequency calculated with respect to $V_{\text{LSR}} = 9 \text{ km s}^{-1}$ (for the Orion compact ridge), except for the CH_3OD rest frequency, which is with respect to $V_{\text{LSR}} = 5.6 \text{ km s}^{-1}$ (representative of the Orion hot core). The rms noise level for the spectral region between U113326 and CH_3OD is 3.7 mK.



L. E. Snyder et al,
Astrophys. J. **619**,
 914-930(2005)

Glycine in Comet Tail

Glycine has been identified in a dust sample collected by the Stardust Spacecraft from the tail of Comet Wild 2.

<http://www.newscientist.com/article/dn17628-found-first-amino-acid-on-a-comet.html>

http://scientificinquiry.suite101.com/article.cfm/comet_tail_with_glycine_amino_acid_amazes_all

In future

- Sub-mm astronomical observations with very high spatial resolution.

ALMA

- In the process of star and planet formation, what kind of molecules can survive and be entrained into the planetary system? Life related molecules?
- Lab. data are essential in such identifications.

*“To understand hydrogen is to
understand all of physics,
chemistry, and biology.”*

Victor Weisskopf

Hydrogen, light colorless odorless gas,
which given enough time
turns into human being

氫，輕質量 無色 無味的氣體，
如果給它足夠的時間
它會逐漸演變成今天的人類



Discovery of multiply deuterated species in space

$$[D]/[H] \sim 1.5 \times 10^{-5}$$

D₂CO : Turner(1990) Ori-KL 0.3%

Ceccarelli *et al* (1998) IRAS 16293-2422 5%

Loinard *et al* (2001) 16293E 26%

NHD₂ (2000) , ND₃ (2002)

CHD₂OH (2002), CD₃OH (2004)

D₂S (2003)

Formation of Deuterated Species

- H/D exchange reactions of H_3^+ with HD are exothermic.



- Under liquid- N_2 cooled environment, such reactions become dominant.

Spectroscopy of H_2D^+ and D_2H^+

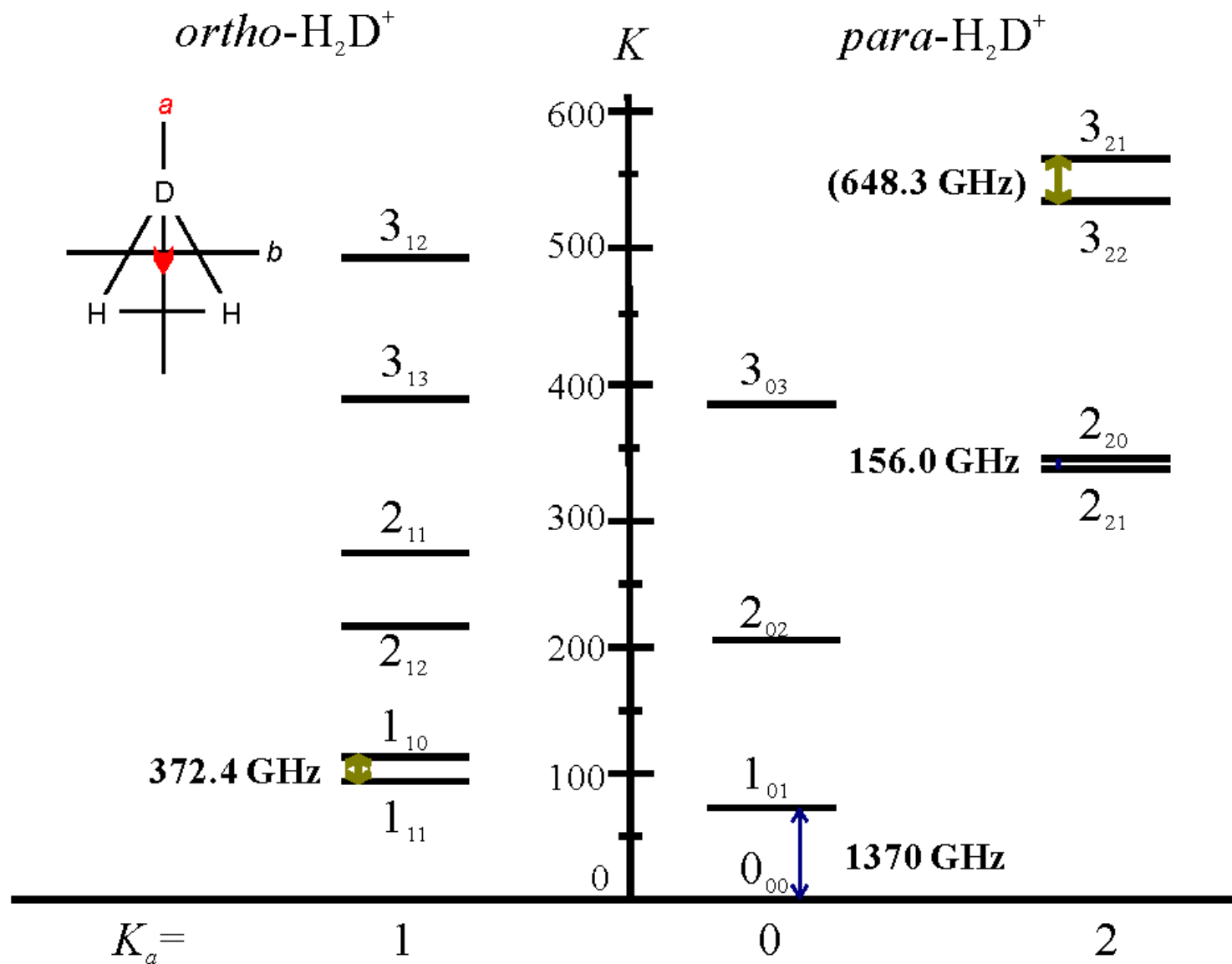
IR

- Shy, Farley, Wing (1981): Ion beam
- Amano & Watson (1984), Amano (1985): ν_1 band (H_2D^+)
- Lubic & Amano (1984): ν_1 band (D_2H^+)
- Foster et al. (1986): ν_2 / ν_3 bands (H_2D^+)
- Foster, McKellar, Watson. (1986): ν_2 / ν_3 bands (D_2H^+)
- Polyansky & McKellar (1990): All available data were fitted together to improve molecular constants. (D_2H^+)
- Fárník et al. (2002):
Molecular beam experiments of vibrational overtone and combination bands ($2\nu_2, 2\nu_3, \nu_2+\nu_3$).

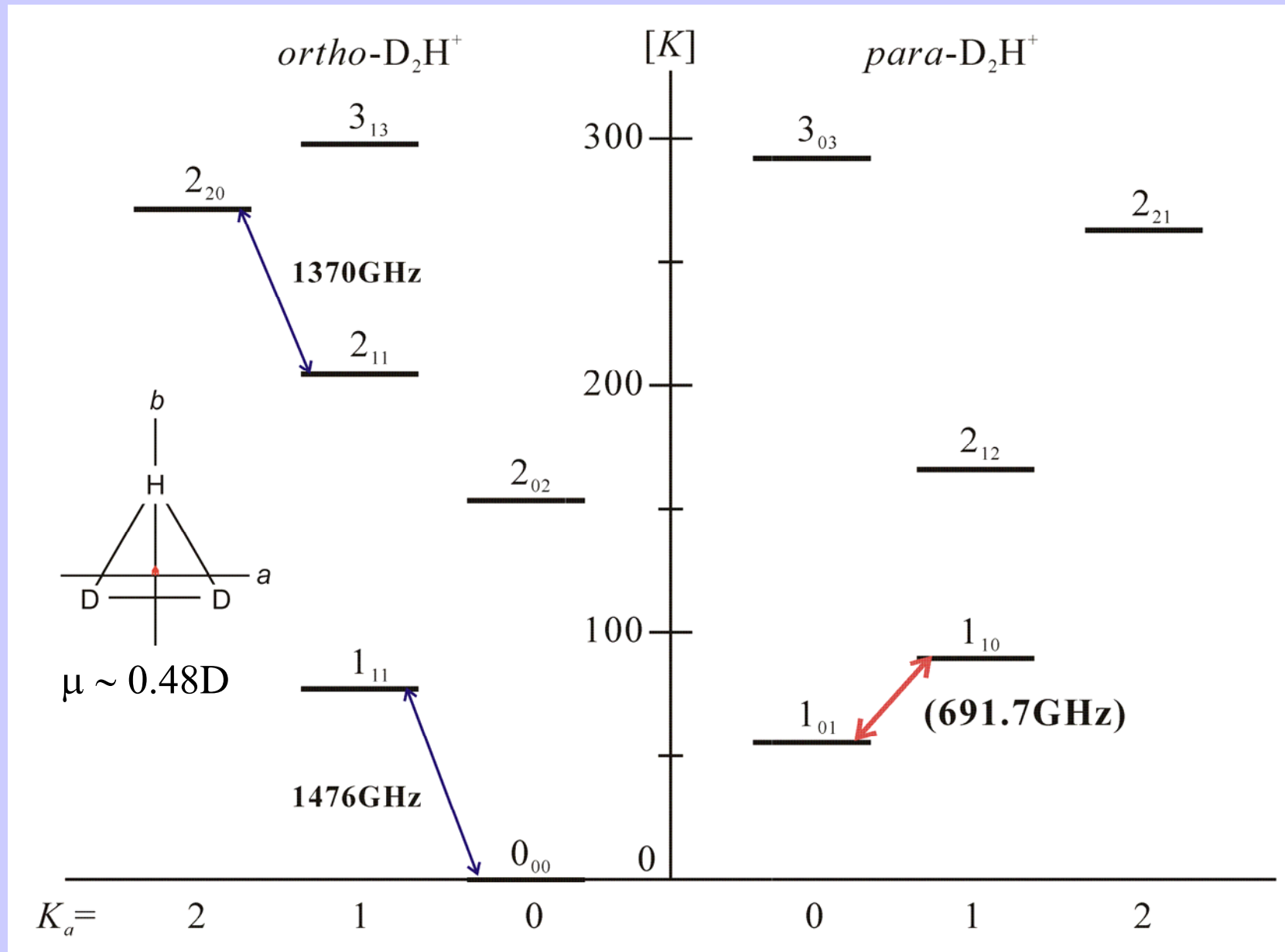
mm-, sub-mm, FIR

- Bogey et al. (1984): $1_{10}-1_{11}$ H_2D^+ (372.4 GHz)
Warner et al.(1984):
- Saito, Kawaguchi, Hirota (1985): $2_{20}-2_{21}$ H_2D^+ (156.0 GHz)
- Jennings, Demuynck, Banek, Evenson (unpublished):
 - $1_{01}-0_{00}$ H_2D^+ (1370.1 GHz)
 - $1_{11}-0_{00}$ D_2H^+ (1476.6 GHz)
 - $2_{20}-2_{11}$ D_2H^+ (1370.1 GHz)
- Hirao & Amano (2003): $1_{10}-1_{01}$ D_2H^+ (691.7 GHz)
- Amano & Hirao (2005): $3_{21}-3_{22}$ H_2D^+ (646.4 GHz)

Energy Level Diagram of H_2D^+



Energy Level Diagram of D_2H^+

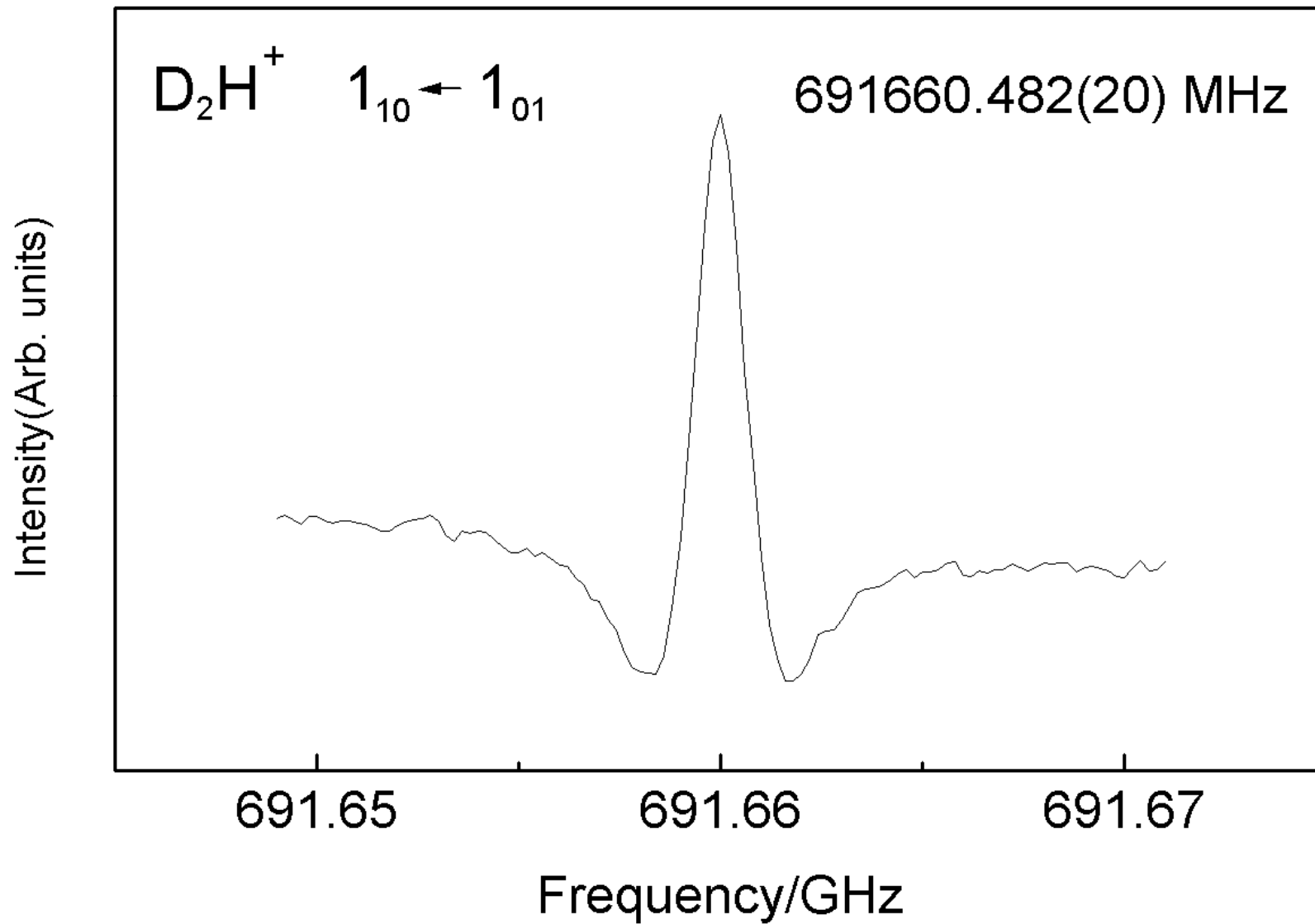


Experimental Details

- Extended negative glow discharge source.
(Magnetic field: 200G).
- Double modulation.
- $\text{H}_2/\text{D}_2/\text{Ar} = 3 / 2 / 17$ mTorr, $I = 8$ mA,
 $T \sim 77$ K



Search around 691.705 (90) GHz.
(Polyansky and McKellar)



T. Hirao and T. Amano, Astrophys. J. Lett. 597, L85(2003).

D₂H⁺ HAS IN

C. Vastel, T. G. Phillips
Ap. J. Lett. **606**

16293E pre-stellar
[D₂H⁺] ~ [H₂D⁺]

- 10 -

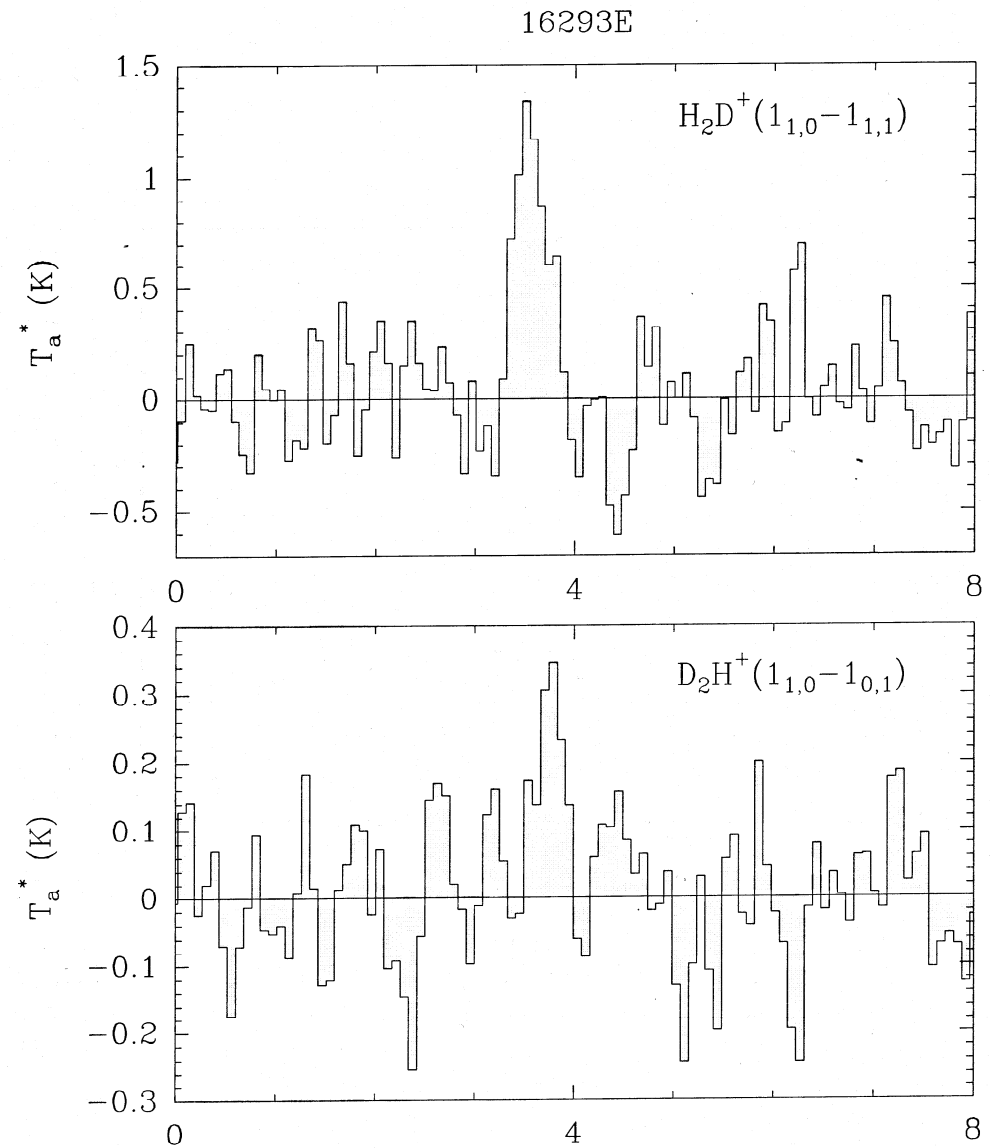


Fig. 3.— Spectra of the ortho-H₂D⁺ 1₁₀-1₁₁ and para-D₂H⁺ 1₁₀-1₀₁ transitions towards 16293E.

Table 1. Results of Gaussian fits to the H₂D⁺ and D₂H⁺ spectra.

Line	ν (GHz)	T_a^* (K)	Δv (km s ⁻¹)	V_{LSR} (km s ⁻¹)
H ₂ D ⁺ (1 ₁₀ -1 ₁₁)	372.42134(20) ^a	1.31	0.36 ± 0.04	3.55 ± 0.02
D ₂ H ⁺ (1 ₁₀ -1 ₀₁)	691.660440(19) ^b	0.34	0.29 ± 0.07	3.76 ± 0.03

^aMeasured frequency by Bogey et al. (1984).

^bMeasured frequency by Hirao and Amano (2003).

⇒ Prompted us to remeasure H₂D⁺ line

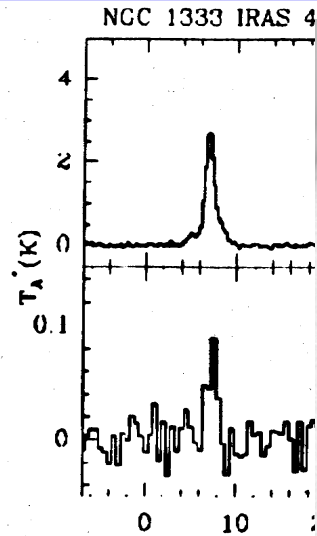


FIG. 1.—Observations of the $\text{H}_2\text{D}^+(1_{10}-1_{11})$ line at 372.672 GHz. The continuum spectra have been subtracted.

Caselli, van der Grinten & Ceccarelli 2003

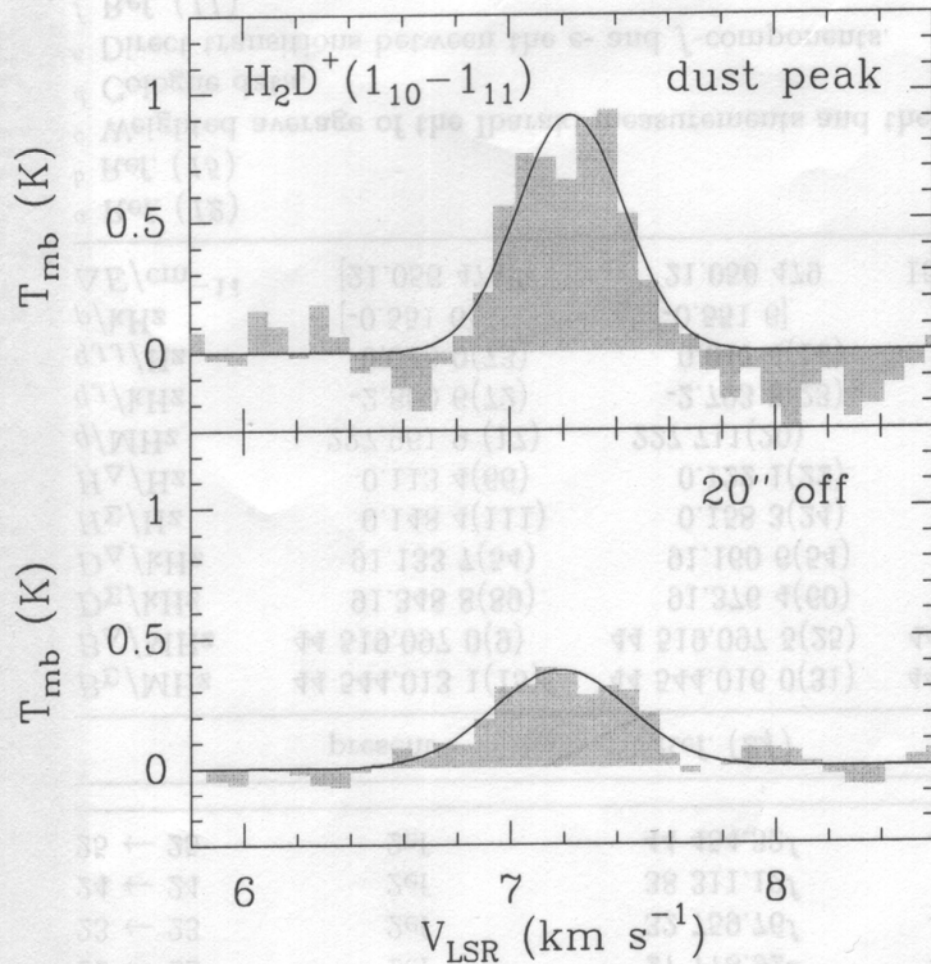


Fig. 1. (Top) The $\text{H}_2\text{D}^+(1_{10}-1_{11})$ line at the dust peak of L1544 (RA(1950) = 05:01:13.1, Dec(1950) = 25:06:35.0). The black curve is the Gaussian fit (see Table 1). (Bottom) The $\text{H}_2\text{D}^+(1_{10}-1_{11})$ spectrum averaged in the four positions 20'' off the dust peak.

003

